Materials Advances

ROYAL SOCIETY OF CHEMISTRY

REVIEW

View Article Online
View Journal | View Issue

Cite this: *Mater. Adv.*, 2025, **6**, 1554

Metal organic frameworks in photodynamic therapy of cancer: functional roles of active metal centres and integrated and loaded photosensitizers in the framework

Temitope O. Abodunrin, *[a] Godshelp O. Egharevba,[a] Fisayo D. Owoeye, [b] Johnson A. Omojola[c] and Oluyomi S. Adeyemi[de]

Cancer is a major health challenge that is accountable for a large percentage of disease-related deaths worldwide. Annually, new cancer diagnoses reach over 10 million with a record of about 9.6 million deaths. Owing to the high prevalence of novel cases and low survival rate of cancer, studies on its diagnosis and treatment are important. Current methods used for the treatment of cancer include surgery, radiotherapy, molecular-targeted therapy, immunotherapy and chemotherapy; each with its own limitations. Photodynamic therapy (PDT) is another method developed for the treatment of cancer from conventional chemotherapy, radiotherapy and surgery. PDT is better than other therapies owing to its non-invasiveness and fast cure process. The challenges of PDT are poor biocompatibility, acidic environment and complex synthetic procedures. To overcome these barriers, metal organic frameworks (MOFs) and their nanoscale metal organic framework (NMOF) counterparts have been incorporated into PDT. MOFs and NMOFs are assemblies of organic ligands and inorganic metal nodes fashioned into ordered networks applied as photosensitizers (PS) or carriers of the same in PDT. The benefits of MOF-based platforms for PDT include their hydrophilic property, high stability, high reactive oxygen species (ROS) utilization and efficient renal clearance. Several MOFs synthesized from hydrothermal, solvothermal, microwave-assisted, sonochemical, ball and liquid-assisted, and mechanochemical milling procedures have been applied for PDT with positive results. However, future research is expected to focus on the design of innovative MOFs and NMOFs that are suitable for various conditions. This review focuses on photodynamic therapy using metal organic frameworks. It discusses the roles and activities of active metal ions/clusters, PS integrated into MOF scaffolds, PS carried in MOF backbone, MOFs integrated with upconversion nanoparticles (UCNP), recent accomplishments, and the future direction of MOFs in photosensitization for photodynamic cancer therapy.

Received 24th April 2024,
Accepted 7th January 2025

DOI: 10.1039/d4ma00425f

rsc.li/materials-advances

Introduction

Cancer has been responsible for a large percentage of disease-related deaths, and is a major global health challenge. Annually, more than 10 million new diagnosed cases are reported worldwide. Its low survival rate calls for expedient research focused on diagnosis and treatment. Several clinical therapies have been applied for its treatment and related cases, including conventional therapies, such as radiotherapy, chemotherapy, immunotherapy, molecular targeted therapy, combined therapies and surgery. However, these treatments have drawbacks that impair their efficacies. Surgery is limited by cancer metastasis or recurrence of certain tumors. Meanwhile, for radiotherapy, radiation poisoning and unwanted damage to surrounding normal tissue are common. For immunotherapy, inconsistent outcomes for different patients are experienced, whereas chemotherapy can cause systemic toxicity associated with side effects, such as alopecia, mucositis, myelosuppression.[1–4]

The modern technology for photodynamic therapy (PDT) has evolved recently as a promising therapeutic method from the conventional approaches of chemotherapy, radiotherapy and surgery for the treatment of cancer.[5] The breakthroughs associated with PDT include minimal invasiveness, which is characterized by negligible systemic toxicity, high selectivity, outstanding therapeutic outcome and very few side effects.[6–8]

[a] *Industrial Chemistry Department, Landmark University, Omu-Aran, Nigeria. E-mail: abodunrin.temitope@lmu.edu.ng*
[b] *Biochemistry Department, Wesley University, Ondo, Nigeria*
[c] *Chemistry Department, University of Ibadan, Nigeria*
[d] *Biochemistry Department, Landmark University, Omu-Aran, Nigeria*
[e] *Biochemistry Department, Bowen University, Nigeria*

Additional benefits of PDT over other cancer therapies include its fast cure process, room for combination therapies, tendency to overcome bacteria and multidrug resistance, and enhanced permeability and retention effect (EPR).[8,9] Some challenges of PDT include its poor biocompatibility, need for an acidic environment, and complex synthetic procedures.[10]

Metal organic frameworks (MOFs) and its nanoscale metal organic frameworks (NMOFs) counterparts are assemblies of organic ligands and inorganic metal nodes fashioned into ordered networks, and have shown promising applications in PDT. For PDT applications, MOFs and NMOFs have been explored as platforms for the introduction of photosensitizers (PS) into pores, specifically as vehicles/carriers for the integration of PS into their backbones for photosensitization.[11] The advantages of MOF-based platforms for PDT include its hydrophilic property, high stability, high reactive oxygen species (ROS) utilization and efficient renal clearance.[12] The use of nanoplatforms overcomes the limitation associated with photoreduction in PDT efficacy caused by tumor aggravation due to oxygen consumption. And, it possesses the ability to produce oxygen through the catalytic decomposition of peroxide.[2]

This review explores recent advancements in the roles of the metal organic frameworks structure in the photodynamic therapy of cancer. The different forms of MOFs common in PDT that have been explored include the pristine MOFs, functionalized MOFs, nano-MOF, MOF composites and up-conversion nanoparticles MOFs. This review details the mechanism of PDT and the roles of the active metal ion/centres in MOFs, MOF backbone with PS integrated into the scaffold, those in which the MOFs serve as carriers of PS, multi-theranostic platforms of MOFs and UCNP MOFs. The resultant PDT outcomes of the different forms of MOFs were discussed, along with various constituents of MOFs. Finally, this review summarizes the limitations of the PDT mechanism that have been overcome by MOFs and the future outlook of this therapeutic approach.

Photodynamic therapy (PDT)

PDT is based on the principle of stimulation of PS to generate highly reactive oxygen species to damage cancerous targets.[13] PDT is safe and effective because it destroys only the affected cells, offering significant reduction of side effects and improvement in target specificity.[2] The treatment of malignant tumors using PDT offers a quick therapeutic effect and reduced damage to normal tissues, while allowing for repeated treatment at the same site, and flexibility with other therapies.[14,15]

Components of photodynamic therapy

The individual components of PDT are non-toxic. A photosensitizer, light and molecular oxygen are the components simultaneously required in the tripartite PDT process, which also influences the production of ROS.[5,16,17]

Light source

PDT entails the use of PS to trigger light of a specific wavelength with low power visible light. PDT is initiated by the light activation of PS, which transfers energy to molecular oxygen for the generation of highly cytotoxic ROS.[18] The light sources that are often employed are harmless, and are accurately positioned to activate therapy.[19] The light source is dependent on the absorption of PS, while the depth of penetration relies on the wavelength of light and its properties, such as absorption, reflection, transmission and scattering.[8,20] Red light sources possess wavelengths between 630 to 700 nm, which corresponds to a light penetration depth that can stimulate PSs. Laser light sources that are currently used for PDT include gallium–aluminum–arsenide diode lasers with wavelengths between 630 to 690 nm or 830 to 906 nm, helium-neon lasers with a wavelength of 633 nm, and argon lasers with wavelengths in the range of 488 to 514 nm. Non-laser light sources such as LED (light emitting diodes) are also an emerging trend in PDT.[21]

Photosensitizers (PS)

PSs are light-activated compounds that act as catalysts to high ROS, such as singlet oxygen and free radicals.[21] PSs are not toxic, but generate reactive oxygen species (ROS) in the presence of light and oxygen, which can induce cell apoptosis through damage to proteins, lipids, nucleic acids, membranes and organelles.[8] The dosage of light applied, location of the tumor, and the selected light source depends on the type and nature of PS that is being utilized.[2] Meanwhile, the efficiency of the PDT system depends on the efficiency of the light conversion ability of the PS and its delivery to the target sites. Hence, PS are the core of the PDT system due to their structural diversity, superior biosafety, and reproducibility.[17,22]

Over 1000 natural and artificial PSs have been discovered, but only a small number have gained clinical applications and are commercially available for the treatment of cancers.[2,23] Effective PSs for PDT can produce highly oxygenated products and singlet oxygen. First generation PSs exhibited long residence times, but were limited by poor tissue penetration depth due to short wavelengths, complex synthetic and purification processes, poor solubility, high administration dosage due to low molar extinction coefficients and prolonged periods of photosensitization due to their long half-life. The second-generation PS possessed enhanced photosensitivity, absorption spectrum and tissue selectivity, but were restricted by their non-specific localization at target cells/tissues. However, recent clinical therapeutics face challenges, such as low target specificity, poor penetration depth of the PSs, complex artificial modification, low payloads, easy aggregation, non-targeted phototoxicity, poor tumor targeting and accumulation competence due to the hydrophobicity of PS. These outcomes have led to insufficient tumor localization, formation of aggregates in physiological environments, and depletion of internally generated ROS by endogenous antioxidants through aggregation-induced quenching.[2,6,22–26] Thus, the efficiency of PSs in PDT is compromised by the presence of photobleaching, low extinction coefficients, dissatisfactory ROS, and poor water solubility.[27]

Mechanism of photodynamic therapy

The mechanism of PDT involves the transfer of an absorbed photon by the PS upon light excitation at an appropriate wavelength to the molecules of oxygen or other substrates in

its surrounding environment for the generation of highly cytotoxic ROS, such as free radicals ($^{\bullet}O_2^-$) or singlet oxygen ($^1O_2$). This process induces irreversible damage to tissues or cells.[28,29] The primary mechanism for PDT results in direct destruction of cancerous cells, tumor infraction as a result of lesions on the tumor-associated vasculature, and systemic immunity, which arises from subsequent inflammatory responses.[3]

Light irradiation stimulates the absorption of a photon by PS I in the ground state, activates the singlet oxygen to an excited state, and then converts PS II into an excited triplet state *via* intersystem crossing. Free radicals such as peroxides and superoxide anions are produced by Type I reaction *via* energy transfer between the triplet excited state and the biological substrate. Meanwhile, the production of singlet oxygen (which is highly reactive oxygen) results from Type II reactions through electron or hydrogen transfer involved in the photochemical reaction, as depicted in Fig. 1.[21,22]

Fig. 1 gives a schematic illustration of the mechanism of the photodynamic reaction process.

The interaction of specific molecules by PS III in the triplet state generates Type I and Type II reactions.[21] The abstraction of hydrogen or the relocation of an electron between either the adjacent molecules or molecular oxygen produces radicals or super oxide anions, respectively, and the PS-excited triplet state in the Type I mechanism is shown in Fig. 2. Hence, hydrogen peroxide at higher concentration reacts with super oxide anions for the formation of highly reactive hydroxyl radicals capable of attacking and oxidizing biological molecules within the cell. Furthermore, Fenton's reaction arises from the interaction between neighbouring metal ions such as copper or iron and superoxide anions to generate hydroxyl radicals. Singlet oxygen produced through the transfer of energy from the PS-excited triplet state to molecular oxygen during collisions is a feature of the Type II mechanism (Fig. 2). Damages are induced by

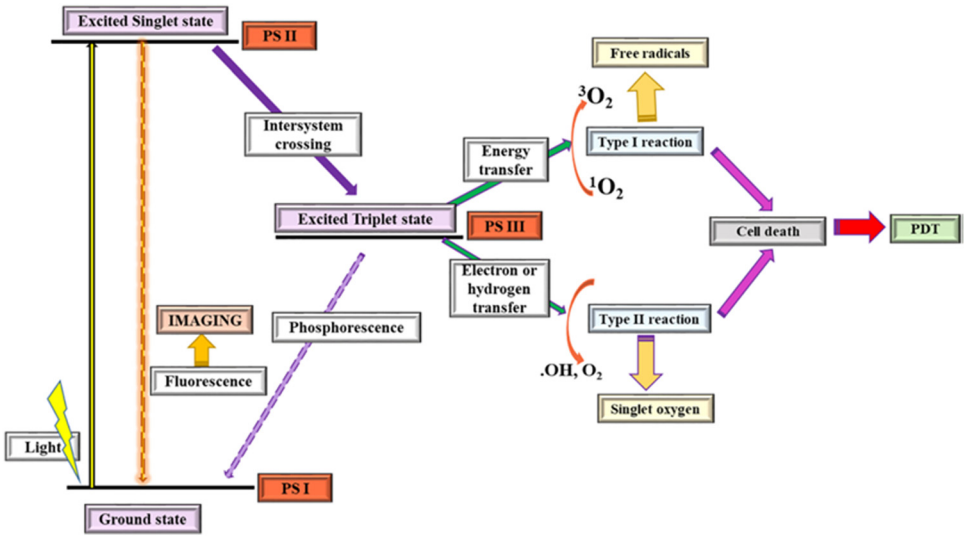

Fig. 1 Photodynamic reaction process (reproduced with permission from ref. 21. Copyright 2019, Elsevier).

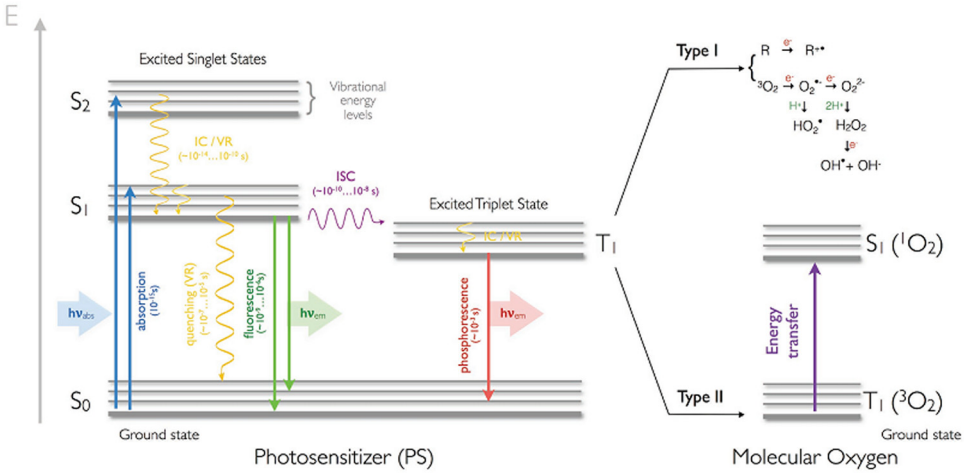

Fig. 2 Jablonski diagram describing the photochemistry and photophysics of PDT. Ground singlet state (S_0), excited singlet state (S_1), internal conversion (IC), vibrational relaxation (VR), and intersystem crossing (ISC) (reproduced with permission from ref. 28. Copyright 2017, Wiley and Sons).

the diffusion of peroxide, hydroxyl radical and singlet oxygen. Type I and Type II photochemical processes occur parallel to one another, and their ratio is a function of the PS used and the available molecular oxygen and organic substrates. Type II mechanisms (in Fig. 2) are typically more common than Type I due to the importance of oxygen at low concentrations for the latter.[28] The Jablonski diagram shown in Fig. 2 summarizes the photochemistry and photophysics of the PDT process.

PDT combines photochemical and photophysical processes to accomplish biological effects. It has great significance due to its potential to overcome treatment resistance, minimal invasiveness and selective treatment, low systemic toxicity, versatility and compatibility with other therapies.[16,30] The induction of the tumor cell death occurs *via* three mechanisms; namely, direct cell apoptosis and/or necrosis, tumor vasculature shut down and immune system activation.[8,15] During multiple PDT mechanisms, the formed reactive species result in the indirect mortality of cancer cells by damage of the tumor vasculature. While cancer cell mortality can occur directly by autophagy, apoptosis, necrosis, as well as inflammation that triggers immunotherapy to accomplish the treatment of cancer.[2,31]

Metal organic framework (MOF)

Metal organic frameworks (MOFs), according to IUPAC, can be described as metal networks with organic ligands containing potential spaces and corresponding coordination, which extend through repeating coordination entities in 1D, 2D or 3D. The porous crystalline scaffolds are assembled periodically, and preserved by robust coordination bonds in the metal ion or clusters identified as inorganic building units (IBU) and negatively charged organic linkers known as organic building units.[28] These are illustrated in the conceptual assembly depicted in Fig. 3.

MOF belongs to a category of recently developed functional materials, which are crystalline and consist of organic linkers and inorganic nodes assembled to form multidimensional lattices through coordination bonds.[32,33] MOFs are constructed from metals/clusters connected by organic linkers like carboxylates, phosphonates and sulfonates that are well ordered to form coordination polymers.[34–36]

MOFs have been constructed with different metal ions, such as alkali metal, transition metal and lanthanide. However, bioinorganic metals found in living organisms, such as Fe, Mn, Cu, Zn ions, have also been utilized due to their biocompatibility. Some MOFs are constructed using metals with active pharmaceutical components such as silver.[37] Hard Lewis acids such as Zr^{4+} and Hf^{4+} have been employed in the fabrication of highly water-resistant MOFs for enlargement of their working environments.[38]

Synthetic methods for obtaining metal organic frameworks

The synthesis of MOFs involves the combination of an appropriate organic linker with an inorganic metal. These can be either in the liquid phase or in the solid phase.[39] Several synthetic procedures that have been used include hydrothermal, solvothermal, microwave-assisted, sonochemical and mechanochemical milling.[40,41] These procedures, along with their reaction conditions and advantages, are given in Fig. 4.

Classes of metal organic frameworks employed in photodynamic therapy

Pristine metal organic frameworks

Pristine MOFs are virgin MOFs that have not been subjected to alteration, chemical modification or functionalization.[42]

Functionalized metal organic frameworks

MOF backbones of pristine MOFs are capable of being functionalized through the addition of more modifications, which allow for the tuning of the physical and chemical properties of the MOF.[43] The functional moieties added into the MOF backbone do not alter the structure of the functionalized MOF.[42] The functions of MOFs can be extended and enriched by diverse ligands and coating materials. Functionalization can be achieved through surface decoration, ligand incorporation, ligand exchange, encapsulation, dopant modification, chemical grafting and entrapment of functional molecules into the framework.[15,37,44] The surface of MOFs can be chemically modified using coordinative binding on unsaturated metal sites, covalent binding to linking groups, pre-functionalized linkers or ligand exchange, *etc.* The availability of numerous sites for modification of MOF for multifunctional clinical applications can be achieved through the assembly of MOF structures with multitudinous biomolecules.[9] Functionalization creates platforms for target and on-demand delivery of therapeutics. It also leads to improvement of the cell uptake

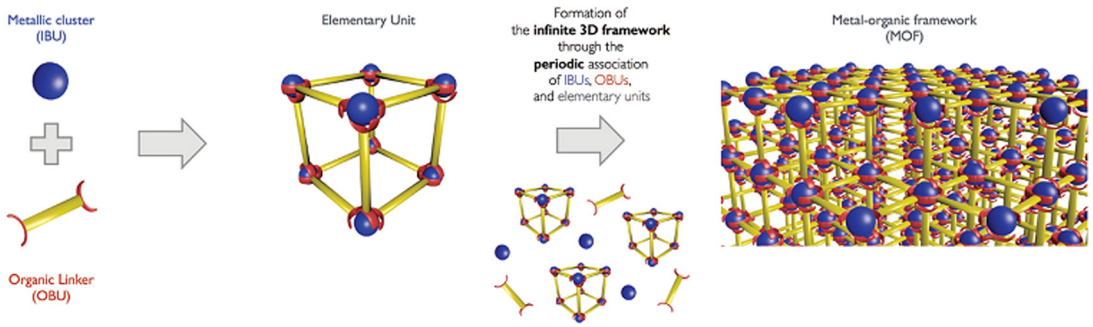

Fig. 3 Conceptual assembly of MOF (reproduced with permission from ref. 32. Copyright 2017, Wiley and Sons).

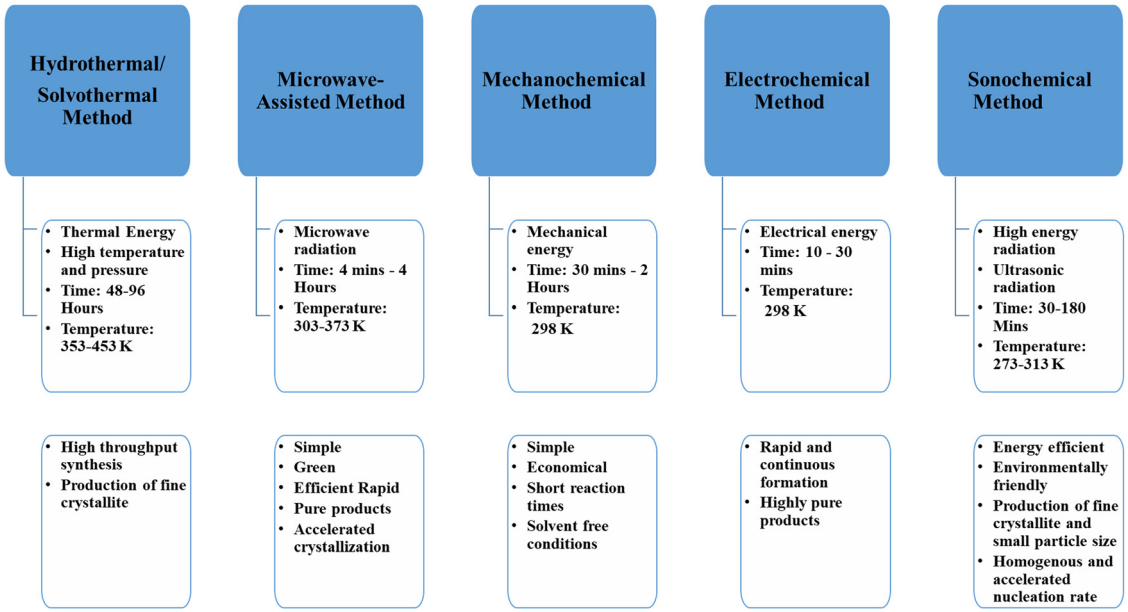

Fig. 4 Summary of synthetic procedures of MOF.

efficiency, cytotoxicity, biostability, drug metabolism and synergistic effect.[37,45] Surface functionalization greatly improves the tumor targeting efficiency.[2,37]

PSs, biomolecules, polymers and functional agents can be utilized for modification. Biocompatibility and stability are improved by surface functionalization of MOFs. However, the cancer targeting ability of MOF can be improved and strengthened by post-modification with target ligands and by conjugation of targeting agents to PS.[2,44] Decoration of target molecules can lead to specific delivery and binding. PEGylation imparts excellent stability in physiological conditions, provides hydrophilic layered coat, shields from the environment, extends the circulation time in blood for distribution to other organs, gives good tumor-targeting ability, increases dispersibility, and prevents aggregation.[37,45–50]

Nano metal organic framework (NMOF)

Nano MOFs (NMOFs) are MOFs constructed in the nanoscale regime by coordination of metal ion bonds and organic linkers.[51] These NMOFs have dimensions that are in the nanometer range.[43] Some of the features of NMOFs include intrinsic biodegradability, high drug loading capacity, structural/compositional tunability, controlled composition, synthetic tunability, flexible functionality, large specific area and ultrahigh porosity.[16,25,27]

In the biomedical field, the application of nanoparticles and their modification with suitable specific functions has received much attention for the treatment of cancer.[34] Nanoparticle materials possess features, such as reduced size, and distinct chemical, photochemical, electronic, magnetic and optical properties.[52]

NMOFs have been utilized as vehicles for the transport of PS, therapeutics and contrast agents in cancer therapy.[53] In PDT, the desired properties of the nanomaterials include their stability under irradiation and improved penetration due to their promising optical properties.[2] NMOFs are utilized as therapeutics, contrast agents and photosensitisers.[53] They are employed in PDT because they offer large surface-to-volume ratios of the materials, employ an enhanced permeability retention effect (EPR), allows for modification of the functional groups, co-encapsulation with other agents, and boost the cellular uptake. These properties account for their ability to prevent pre-mature leakage of PS, increase the delivered quantity of PS, and alter the biological and physical properties for optimum biodistribution, pharmacokinetics, tumor accumulation, cell entry, and inclusion of multifunctional platforms that are beneficial and accomplish heightened build-up for cancer directed imaging and treatment.[15,23,50] The use of nanoplatforms overcomes the limitation associated with a reduction in PDT efficacy caused by tumor aggravation *via* oxygen consumption. Nanoplatforms possess the ability to produce oxygen through the catalytic decomposition of peroxide.[2,53]

Metal organic framework composites

MOF composites are multi-component materials with multiple phases, which consist of individual constituent materials integrated into MOFs to improve its properties. Such MOFs possess better properties than its starting materials.[43]

MOF-based composites are produced when the pore spaces on MOFs lodge multiple additional active species as guests.[54] They also are formed as products of polymer integration. Post-synthetic modification of MOFs with polymers can be used to impart specific functions, such as stimuli-responsive drug release activity. MOFs modified with polymers are endowed with stimuli-responsive drug release activity.[37,49,55]

Upconversion nanoparticles (UCNP) MOF

Upconversion nanoparticles (UCNP) are functional NPs of less than 100 nm diameter possessing anti-Stokes emission.[1] These photoconverting transducers change near-infrared light to shorter near-infrared or ultra-visible light for the activation of

PS.[23] In UNCP, more than one photon with relatively low energy is absorbed and converted to higher energy photons. This results in the direct transfer of oxygen for the production of ROS and stimulation of PS for exertion of the PDT effect.[14] Integrating UCNP with MOFs combines the photo-upconverting properties of UCNP with the physiochemical properties of MOFs to build an energy transfer system that imparts fascinating optical properties and functionalities.[56]

Metal organic frameworks in photodynamic therapy

MOFs employed for biomedical applications usually possess good biocompatibility, biodegradability and suitable size.[53,57] Biomedical applications of MOFs require that they possess robust stability in the aqueous phase.[38]

MOFs have been utilized in cancer treatment as therapeutics, vehicles for the delivery of cargos such as PSs, enzymes, nucleic acids, active pharmaceutical agents (APIs), *etc.*[19] The contribution of MOFs to the cytotoxic effects on cancer cells is due to their possession of stable crystalline structures, which give room for the integration of a large number of photosensitizers for the generation of singlet oxygen under light. Intersystem crossing of the photosensitizer is facilitated by the heavy metal-based nodes, while the efficiency of oxygen generation is determined by facile diffusion.[57]

The general properties exhibited by MOFs are its specific surface area, higher porosity, and excellent thermal and chemical stability.[30] Nevertheless, MOFs platforms are used in PDT for the following reasons:

(i) For encapsulation or attachment of PS to reduce aggregation of small molecules of PS for singlet oxygen generation.

(ii) To stimulate oxygen diffusion.

(iii) For enhancement of solubility for improved PS uptake.

(iv) To tune the physiochemical properties of various complex conditions.

(v) For combined treatment, which is facilitated by their porous structure and ease of modification.

(vi) For their good biodegradability, significant biocompatibility and low long-term toxicity to organisms.

(vii) Ability to incorporate biocompatible moieties and targeting ligands with the carrier.

(viii) Extensively high retention ability for the release of therapeutics, and their responsive features.

(ix) Specific molecular targeting.

(x) High permeability.

(xi) Efficient cellular uptake.[1,58]

Metal organic frameworks with integrated photosensitisers employed in photodynamic therapy

Metal organic frameworks with active metal ions/centres in PDT

The coordination strength of the metal ion to the coordinating organic ligand determines the strength of the structure of MOF.[50] The reduction of the metal ion in the MOF generates a super oxide radical anion that is responsible for the damage of cells, and for inducing cancerous cell apoptosis. As in PB@Ti-MIL-125, reduction of Ti(IV) to Ti(III) generated superoxide radical anions for damaging cells and induced cancerous cell apoptosis.[59] MOFs integrated with metal ion/clusters have been shown to maximize their antitumor efficacy, and are better in terms of targeting, accumulation and site retention. Such MOFs exhibit intelligent responses as a function of the oxidation power of the metal ion/cluster. The coordination of Mn(III) to TCPP produced a system where the Mn(III) served as a sealer, which locked the theranostic function and inhibited ROS generation (Fig. 5).[25] Also, the improved physiochemical properties and enhanced intersystem crossing, which causes three-fold ROS generation, are imparted by the presence of heavy metal nodes, as seen in Sm-H_2TCPP. The regular isolation of the metal node prevents self-quenching induced aggregation in the energized state, which leads to the local conjugative effect responsible for the reduction in the energy gap from the triplet to singlet excited state.[27] Also, the employment of a high z-element in NMOFs increases the functionality of such MOFs to include radiotherapy application. The presence of Hf ions in Hf-TCPP NMOF PEG is responsible for the production of free radicals that destroy cancer cells when photo/auger electrons interact with ionizing radiation.[50]

Pristine metal organic framework employed as PS in PDT

MOFs that function as PS possess photosensitive and photochromic metal ions or organic linkers. These materials are integrated into the MOF scaffold during the formulation of efficient building units. Hence, the linker or metal ion will be tasked with the responsibility of generating the singlet oxygen required for PDT.[12,15,50] Ligands with photosensitizing properties facilitate the production of sensitized singlet oxygen for distinct ROS, including superoxide ion, hydrogen peroxide and hydroxyl radicals.

PS incorporated directly into the MOF scaffold achieve a well-ordered disassembly of hydrophobic PS molecules for efficient PDT. A nanoscale scaffold has been used for the disassembly of hydrophobic PS to preserve its monomeric state in aqueous solution for the effective delivery of PS and enhanced PDT.[16] They also increase the loading capacity and availability of the PSs. Hence, their photoactivation generates ROS for PDT when in contact with oxygen. They are characterized by the possession of increased extinction coefficients, photostability and therapeutic efficiency.[12,15,23,24] The constituents of these MOFs and the photodynamic conditions for their applications are summarized in Table 1. The photo-redox properties of ligands are responsible for their utilization as PS, especially porphyrin-containing ones. TCPP can function as a PS in the PDT.[58] Usually, their anticancer efficiency can lead to increased tumor regression and cure rate arising from the transfer of excited electrons from the ligand radical to the metal centre.[50,59] Lu *et al.* utilized DBP-UiO and its cholin derivative DBC-UiO as PS. The diffusion of ROS was facilitated by the platelike porous structure of the NMOFs. The coordination of

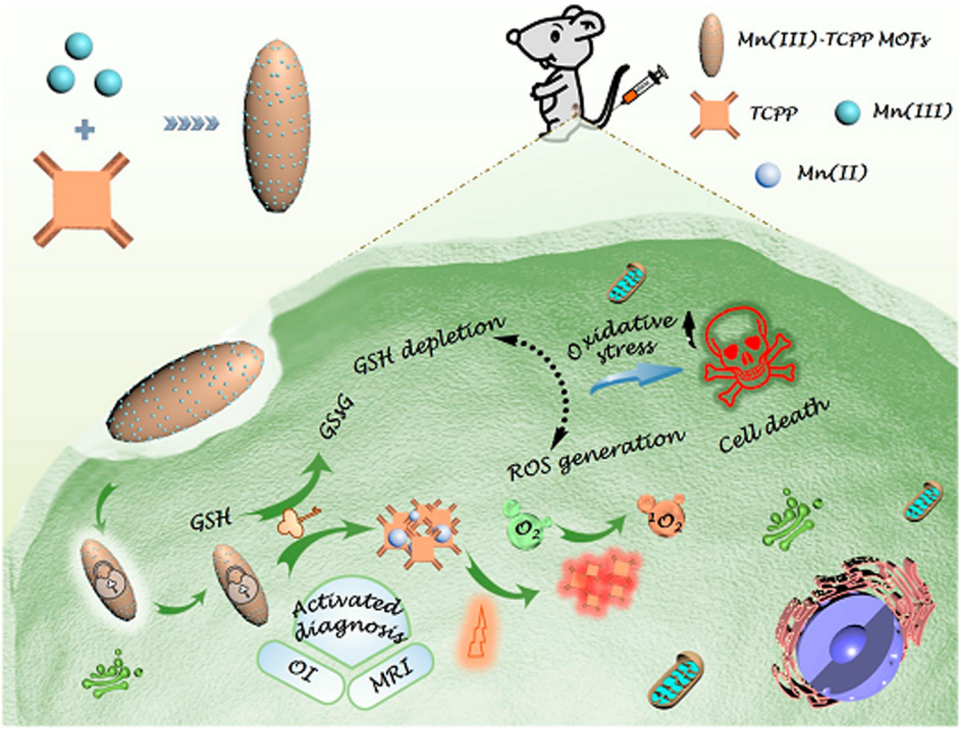

Fig. 5 Schematic representation of a Mn(III)-sealed MOF nanosystem for OI-guided PDT by controlled ROS generation and GSH depletion after being unlocked by overexpressed GSH in tumor cells (reproduced with permission from ref. 25. Copyright 2019, American Chemical Society).

the ligands to Hf^{4+} was responsible for the enhancement of the intersystem crossing (ISC) that generated high singlet oxygen efficiency.[60] In Ti-TBP, with 5,10,15,20-tetra(*p*-benzoato) porphyrin (TBP) as the photosensitizing ligand and Ti-oxo chains as the secondary building unit (SBU), the anticancer efficiency occurs as a result of the transfer of excited electrons from the radical TBP ligand to the Ti centres to generate ROS, which leads to a tumor regression rate of more than 98% and a 60% cure rate.[61] Ti-MIL-125 served as a PS agent in PB@Ti-MIL-125 due to its photo-redox properties. Here, an electron is transferred from the excited ligand to the Ti–O oxo clusters, and interacts with molecular oxygen to produce the superoxide radical anion responsible for cell damage and induction of apoptosis.[59] Under laser irradiation, regular porous porphyrin-based MOF structures facilitate single oxygen generation for PDT, which are effective to prevent the self-quenching of the porphyrinic photosensitizer and the facile oxygen molecules diffusion.[62] Mn–porphyrin ligands and biocompatible Zr^{4+} used to create a porous MOF nano-platform was applied as a guide for magnetic resonance imaging and self-supplemented oxygen PDT. The nanoplatform assembled from the Mn–porphyrin ligand was connected by Zr_6 clusters. Its high-water affinity and the considerable dispersibility of Mn^{3+} in the open channel were responsible for the high longitudinal relaxivity of PCN-22(Mn) at $\sim 35.3\ mM^{-1}\ s^{-1}$ (1.0 T). The good catalytic properties were responsible for conversion of endogenous hydrogen peroxide into oxygen and the improvement of tumour hypoxia during PDT.[62]

Functionalized metal organic frameworks integrated with PS employed in PDT

Grafting of PS with good chelating function to MOF results in external surface decoration of the MOF, which prevents aggregation, enhances the cellular uptake at tumor sites in PDT, while the structural integrity and photosensitivity of the MOFs are preserved. The ROS produced by such MOF in biological systems is characterized by high reactivity and a short half-life which addresses the drawbacks shown in hydrophobic PS.[63]

Organic entities can be used to functionalize MOF for stability in PBS, which can be initiated by the introduction of polyethylene glycol (PEG) and folic acid (FA). The outcome gives an intact crystal structure and morphology with low toxicity and excellent PDT effect.[12] The photophysical properties of TCPP can be improved with PEGylation of the MOF, which imparts exceptional stability in physiological solutions, improved *in vitro* cytotoxicity, long circulation time in blood and efficient tumor targeting.[50] It was observed that the porphyrinic linker demonstrates theranostic modality. Nanoscale PCN-224 possesses astonishing chemical stability with nano-porous channels that facilitate efficient singlet oxygen diffusion. The NMOF also show increased cellular responses that were dependent on the size upon irradiation. However, functionalization with folic acid enhanced the PDT efficiency through active targeting.[64] The use of PEGylated QDs with PCN-224 produced a definite crystal structure, which generated two-fold effective toxic ROS with better performance, displayed rapid renal clearance and tumor accumulation.[12] Post-surface functionalization with FA

Table 1 Properties of MOFs as PS for PDT

MOF	PS	Others	BET	Pore size	Diameter	Zeta ζ	λ and intensity	Time	[PS]	Cells type	Ref.
Ti-TBP	TBP	—	527.7 $m^2\ g^{-1}$	20 nm	100 nm	0.50 V	650 nm 100 mW cm^{-2}	15 min	20 μM	CT26	60
Mn(III) TCPP	TCPP	—	169.9 $cm^2\ g^{-1}$	NA	170 nm	NA	660 nm 0.03/0.22 W cm^{-2}	8 min	20 mg L^{-1}	CT26 3T3 B16	25
PB@Ti-MIL-125	Ti-MIL-125	—	NA	NA	NA	NA	NA	30 min	200 μg mL^{-1}	HePG-2 HL-7702	59
Sm-H_2TCPP	TCPP	—	363.55 $m^2\ g^{-1}$	83.92 nm	NA	−10.9 mV	660 nm 100 mW cm^{-2}	5 min	30 μM	MCF-7	27
Sm-H2TCPP-Pt/TPP	TCPP	CAT TPP-PEG-COOH Nanozyme	NA	∼100 nm	∼100 nm	13.9 mV	660 nm 100 mW cm^{-2}	15 min	50 μM	MCF-10A MCF-7	92
UiO-66-TPP-SH TCPP⊂UiO-66	TPP-SH TCPP	PEG	1260 $m^2\ g^{-1}$ 1051 $m^2\ g^{-1}$	NA	142 nm 140 nm	*ca.* −15 mV	660 nm 100 mW cm^{-2}	10 min	0.56 μM 0.56 μM	HeLa	62
Hf-TCPP NMOF-PEG	TCPP	PEG	NA	NA	∼130 nm	−10.16 mV	661 nm 5 mW cm^{-2}	30 min	80 mg L^{-1}	4T1 HeLa NIH3T3	50
MOF QDs	PCN-224 QD	PEG	2316.4 $m^2\ g^{-1}$	4 nm	4.5 nm	−15 mV	650 nm 1 W cm^{-2}	10 min	25 μg mL^{-1}	HeLa	12
NT@PEG@FA	TCPP	PEG FA	1853 $m^2\ g^{-1}$	160 nm	100 nm	−20.9 mV	650 nm 50 mW cm^{-2}	5 min	100 μg mL^{-1}	HeLa	93
PCN 224-FA	TCPP	FA	NA	190 nm	189 nm	20.7 mV	630 nm 100 mW cm^{-2}	30 min	20 μM	HeLa A549	63
ZrMOF-aptamer-TAMRA	TCPP	Aptamer	NA	>110 nm	NA	28 mV	650 nm 200 mW cm^{-2}	5 min	25 μg mL^{-1}	HeLa	64
PCN-PL PCN-PL-@CM	TCPP	PL CM	NA	200 nm	2.7 nm	27 mV −24 mV	660 nm 20 mW cm^{-2}	8 min	12 mg mL^{-1}	3T3 CT-26	82
HA-Dox-PCN	TCPP	HA DOX	1353 $m^2\ g^{-1}$	1.9 nm	∼250 nm	−34 mV	Sunlight 100 mW cm^{-2}	30 min	10 μg mL^{-1}	Hek 293T MDA-MB-231 SCC-7	67
PCN-224-Pt	TCPP	Pt-NP, PEG	NA	90 nm	160.1 nm	NA	638 nm 1 W cm^{-2}	10 min	2 mg mL^{-1}	HeLa 4T1 RAW264.7	57
DOX@PCN-224 DOX@PCN-224-DNA	TCPP	DOX Aptamer	NA	198 nm	230 nm	−20 mV −47 mV	650 nm 100 mW cm^{-2}	15 min	100 μg mL^{-1}	A549 MCF-7 LO2	44
UiO-AM UNM	H_2P	Polyaniline Terephthalaldehyde	1059 $m^2\ g^{-1}$ 974 $m^2\ g^{-1}$	2.5 Å 5 Å	165 nm 176 nm	—	450 nm 45 mW cm^{-2}	15 min	25 μg mL^{-1}	HepG2 HeLa	69

Key: PS-photosensitizer, others: other constituents, BET: surface area, zeta ζ: surface potential, λ: wavelength, time: time of exposure, [PS]: concentration of PS.

resulted in an inbuilt active targeting modality due to coordination of the Zr clusters to the carboxylate end of the folate. The FA functionalization is affected by the size of the nanoparticles. Overall, the functionalized nanoplatform and FA modification play a crucial role in the improvement of the cellular response.[64] MOF NPs anchored on a solid phase DNA-prepared phosphate terminal aptamer served as PS due to the presence of strong coordination, and also as a quencher when π–π stacking was induced. These properties were responsible for its biostability under psychological conditions and target-induced PDT.[65] However, modification of PCN-224 with the aptamer of A549 cells at the carboxyl and fluorescein terminals leads to strong attraction, extraordinary specificity, good direct target therapy and recognition for the cancerous cells.[44]

ZnDTPP-I_2 doped with UiO-66 NMOF to give ZnDTPP-I_2⊂UiO-66 is an efficient nano PS for *in vitro* PDT for cancer cells therapy. Aggregation, which can cause quenching, was effectively prevented by the dispersion of ZnDTPP-I_2 in UiO-66. The presence of iodine atoms in the MOF was responsible for its singlet oxygen generation under physiological conditions. Meanwhile, the release of singlet oxygen was facilitated by the UiO-66 framework.[66]

Metal organic framework composites employed in PDT

Pluronic F127 possesses high hydrophilicity, extractability, and a molecular weight that imparts good biocompatibility.[37,49] A continuous phospholipid bilayers (PBLs) coating on the MOF surface serves as a mimetic membrane to protect the metal nodes from being attacked before they reach the metal sites. This increases the cellular uptake efficiency and improves the biostability.[37,49] The presence of modified cell membranes in the outer layer of the hybrids improves the biocompatibility and promotes a cancer targeting effect *via* active cell–cell adhesion.[67] Thus, MOFs coated with cell membranes for PDT have enhanced blood retention time, stability and immune evading capacity.[37,49] NPs encased by cell membranes impart tumor targeting efficiency, and provide a platform that integrates immune evasion, prolonged circulation time and excellent biocompatibility.[67] The incorporation of hyaluronic acid (HA) on the surface of MOF provides good colloidal stability, keeps drug molecules within the pores, and targets overexpressed receptors that are responsible for efficient internalization by tumors.[68] Folic acid (FA) is used for tumor active targeting, while other targeting molecules (such as aptamers) recognize and bind with tumor cells.[37,49] Also, NPs conjugated with target ligands (such as peptides, antibodies, aptamers, and small molecules) enhance cellular uptake.[65] Usually, DNA aptamers are applied for the assembly of tumor-homing nanocarriers with the ability to bind specifically to the tumor-overexpressed proteins.[67] Additionally, the biocompatibility of MOFs can be enhanced through coupling with biomolecules such as silane.[37] Silica NPs can undergo chemical functionalization due to the presence of hydroxyl groups on the surface of silica.[2] The non-toxicity, optical transparency and chemical inertness are properties of silica nanoparticles that inform their application in the encapsulation of PS in PDT.[69] Low toxicity, increased stability, significant biocompatibility and strong photoluminescence quantum yield are features that make g-C_3N_4 desirable for biomedical applications.[2]

MOF composites can provide intelligent therapeutic outcomes in PDT. MOF composites derived from nanozymes possess efficient PDT and chemo results. Platinum nanozymes have been decorated with photosensitizers integrated on PCN-224 MOF *via in situ* reduction. The MOF, which was homogenously immobilized with platinum nanoparticles, possessed increased stability and catalase activity. The aggregation of neighbouring Pt nanoparticles was hindered and the stability was kept under control by the MOF. The enhanced photodynamic therapy was facilitated by the formation of $^1O_2$ in the hypoxic tumor site *via* hydrogen peroxide-activated evolution of oxygen. The coordination capability of the nanoconjugates decorated with PEG improved the biocompatibility and physiological stability. The formation of cytotoxic $^1O_2$ by PCN-224-Pt for mortality of the cancerous cells was due to the high catalase-like action induced by the breakdown of H_2O_2.[57]

A photoactive MOF@POP nanocomposite was prepared by epitaxial growth of photoactive porphyrin POP (H_2P-POP) on the external surface of the amine-containing UiO-66 (UiO-AM). The amine sites on the external surface of the designated UiO-AM seeds and the feeding ratios of H_2P and terephthaldehyde were set to regulate the size distribution and morphology of the core–shell nanoparticles. The porphyrin-POP-MOF (UNM) is characterized by the regulated size distribution and morphology of the core–shell nanoparticles. UNM satisfactorily retained the crystallization, pore structure and size distribution. The effectiveness of the PDT initiates photo-induced apoptosis of cancer cells. Its capacity to produce efficient singlet oxygen in different experimental environments is influenced by its activation by light.[70]

Metal organic framework employed as carriers of photosensitisers in photodynamic therapy

MOFs serve as vehicles in PDT for the transport of therapeutics into cancer cells. The well-defined MOF structure hosts the relatively isolated PS. Here, the PS is a guest that is carried within the MOF structure, leading to the presence of strong host–guest interactions within the pores of MOFs responsible for their smart property.[12,15,28] Photosensitizers can be loaded into MOFs by direct incorporation as bridging ligands, post-synthetic ligand exchange, postsynthetic surface modification and physical loading into pores. Improvement of the cellular uptake, and the reduction of aggregation and photodegradation are effects of the confinement into lipophilic pores.[71] The diverse structure of MOFs, high specific area, high density and uniform dispersion of active sites are required for availability, effective transport and diffusion of PSs in PDT. In addition, their open structures and many channels facilitate the entry of small substrate molecules and contact with active sites.[12,54]

The organic linkers in the scaffold of MOFs can incorporate active therapeutic agents. The integration of adaptable PSs as ligands or linkers in MOFs makes them attractive carriers for

PDT. These agents are released by degradation of the MOF, which prevents the premature leakage and accumulation of chemotherapeutics. Also, their confinement into nanoscale pores improves their photophysical properties, which enhance the advanced theranostic applications of MOF.[51,72] The degree of loading of a guest is facilitated by the suitability of the internal pores of the MOF to fit the morphology of the guest molecule.[73] MOFs that are used as carriers of PS are characterized by enhanced drug loading efficiency, improved uptake by cancer cells due to the target delivery of PS to the tumor site, increased surface area, and flexible surface variations.[2,23] The porous structure and large surface area of MOF are responsible for its extreme PS loading capacity, biodegradability and the facile diffusion of ROS.[69,72] Similarly, the functional constituents of MOFs are responsible for their utilization as carriers and agents that can be extended and enriched by diverse ligands and coating materials. Thus, MOFs that possess unique features and functionalities from specific backbones are more efficient carriers.[37] Table 2 summarizes the constituents of these MOFs and the conditions in which they have been applied.

Pristine metal organic framework as employed carriers of PS

PS can be separated and maintained in its monomeric state when MOFs act as vehicles and molecular cages protecting against self-aggregation for the generation of cytotoxic singlet oxygen. This is depicted in ZnPc@ZIF-8, which possesses tremendous luminescent intensity due to the presence of zinc(II)phthalocyanine (ZnPc) as a guest, high singlet oxygen production, and PDT activity towards HepG-2 cancer cell lines. The MOF nanoparticles exhibit low cytotoxicity and full biodegradation.[16] Zinc phthalocyanine in the pores of Hf-QC (QC = 2″,3′-dinitro-[1,1′:4′,1″;4″,1‴-quaterphenyl]-4,4‴-dicarboxylate) NMOF also significantly prevented aggregation-induced quenching, improved ROS production, and efficiently regressed cancer cells.[71] In MIL-101(Fe)@TCPP, the biocompatible and biodegradable carrier MIL-101(Fe) functioned as a Fenton nanocatalyst for the conversion of OH radicals from peroxide in acidic environments and as a biocompatible and biodegradable nanovehicle for the delivery of TCPP, while TCPP served as PS that activated the generation of singlet oxygen. TCPP was covalently bonded to the surface of MIL-101(Fe), which enabled *in situ* singlet oxygen generation from specific light activation which resulted in significant suppression of tumor growth *in vivo* with high biosafety. This synergistic therapy resulted in induction of amplified oxidative damage, enhanced PDT, and therapeutic effects without severe side effects.[2,74]

Functionalized metal organic framework employed as PS carriers

The PDT effect, production of singlet oxygen, and intersystem crossing are influenced by the introduction of heavy atoms into PS and MOF nanoparticles.[66] ZIF-90 served as a PDT agent, while iodine-attached BODIPY served as the guest in 2I-Bodipy-$PhNO_2$@ZIF-90, as shown in Fig. 6. As a result, the MOF system possessed low cytotoxicity, good biocompatibility, selective pH driven cancer cell uptake/release, mitochondria targeting, and very efficient pH-triggered singlet oxygen generation. Due to its high performance as a PDT agent, it can be used for the selective destruction of tumor cells.[73]

The presence of more than one PS provides a synergistic relationship between the photosensitizing molecules that lead to a positive influence on the PDT activity. In PCN-I_2BDP, PCN-222 and BODIPY(BDP) serve as PSs and form a single MOF with enhanced light harvesting properties that prevent the self-quenching of PS, which is highly efficient in PDT. The effect of the heavy atom in the MOF leads to the production of a sufficiently populated excited state for PDT, and intersystem crossing that shortens the fluorescence lifetimes.[18] Also, Lu@CoTCPP(Pd) is integrated with an inner light source comprising luminol and H_2O_2, which serves as light. The cobalt SBU catalyses the system, and Pd-metalated porphyrin serves as a photosensitive bridging ligand in the structure, whereas the luminol and H_2O_2 impart chemiluminescence. The incorporation of the heavy atoms of Pd into the porphyrin MOF extend the triplet state lifetime, leading to increased oxygen generation. The MOF system is highly selective with no limitation in therapy depth, and is effective for the mortality of cancerous cells.[5] The incorporation of UiO-67 into $Ru(bpy)_3^{2+}$ (ruthenium(II) tris(bipyridyl) cationic complex) serves as a theranostic platform, which consists of two-photon luminescence intensity and two photon absorption fluorophores. The stearic confinement effect of UiO-67 nanoparticle pores improves the fluorescence intensity of the $Ru(bpy)_3^{2+}$ guest molecules, the luminescence lifetime and the quantum yield. This pathway enhanced the PDT and two-photon fluorescence imaging.[51]

Metal organic framework composite employed as carriers of PS

MOFs can lodge multiple additional active species as guests using pore spaces in their frameworks for the formation of MOF-based nanocomposites. Their pores stabilize the metal NP composite from aggregation, thereby increasing and strengthening their catalytic activity. MOF-based nanocomposites can impart stronger stability and higher activity.[54] The integration of photosensitive components into MOF exerts an increased PDT effect.[58]

Cu(II) MOF was designed with a highly porous feature, nanoscale pores, and a window size large enough to accommodate PS loading. MOF-199 served as a passive carrier for PSs encapsulated in F-127 to increase its dispersibility and biocompatibility, as shown in Fig. 7. Intracellularly, the Cu(II) metal centres functioned as an activator switch for the release of PS and scavenging reagent for the depletion of GSH by the concomitant decomposition of endocytosed MOF and recovery of ROS generation. The *in vitro* and *in vivo* studies on PS@MOF-199 NPs demonstrates its highly efficient cancer ablation and anticancer PDT with diminished normal cell phototoxicity.[24] Gd[PC]@ZIF-8, a smart nanoprobe for synchronous oxygen sensing and PDT, contained a homogenous oxygen-sensitive phosphor complex Gd[$(Pyr)_4$cyclen] and a rare earth metal that was encapsulated into ZIF-8. ZIF-8 nanocarriers efficiently delivered hydrophobic Gd(III) into the cells. The PS-Gd[$(Pyr)_4$cyclen] favourably converted sufficient oxygen molecules into single state oxygen when irradiated during the phosphorescent quenching process for PDT.

Table 2 Properties of MOFs as carriers of PS for PDT

MOF	PS	Others	BET	Pore size	Diameter	Zeta ζ	λ and intensity	Time	[PS]	Cells type	Ref.
2I-Bodipy $PhNO_2$@ZIF-90	2IBodipy $PhNO_2$	—	NA	11.2 Å	<80 nm	−12.5 to 8.7 mV (pH 7.4, 7.0, 6.5 and 5.9)	540 nm 20 mW cm^{-2}	8 min	20 μg mL^{-1}	HL-7702 HepG2 MCF-7 MCF-10A	72
ZnPc@ZIF-8	ZnPc	—	NA	342.0 nm (pH 7.4) 190.1 nm (pH 5.0)	NA	NA	650 nm 3.3 mW cm^{-2}	10 min	50 μg mL^{-1}	MC3T3-E1 HepG2	16
PCN-222 PCN–I2BDP	TCPP TCPP, BODIPY	—	1755 m^2 g^{-1} 1015 m^2 g^{-1}	80 nm	NA	NA	36 W (LED light) 4 mW cm^{-2}	3 h	5μM	MCF-7 B16F10	18
ZnDTPP-I2 ⊂ UiO-66	ZnDTPP	—	901 m^2 g^{-1}	85.5 nm	110 nm 6.7 Å	NA	540 nm 20 mW cm^{-2}	10 min	0.55 μM	HepG2	65
Lu@CoTCPP(Pd) (nUiO-67)-Ru(bpy)$_3^{2+}$	Pd-TCPP Ru(bpy)$_3^{2+}$	Luminol —	NA NA	3.8 nm 218 nm	100 nm 92 nm	NA 7.0 mV	400 nm Xenon lamp 200 mW cm^{-2}	NA 10 min	NA 25 μg mL^{-1}	SKOV3 A549	5 51
Gd[PC]@PVP Gd[PC]@ZIF-8 Gd[PC]@ZIF-8@PLL	Gd[PC]	PLL	806.12 m^2 g^{-1}	20 nm 200 nm	NA	−4.69 mV +2.53 mV +1.89 Mv	365 nm	15 min	NA	HeLa	74
PCN-CuS-FA-ICG	ICG	CuS NP FA PVP	NA	NA	112 nm	5.1 mV	650 nm 50 mW cm^{-2}	5 min	200 μg mL^{-1}	MDA-MB-231	76
P@Pt@P-Au-FA	PCN	Pt NP PVP Au NP FA	NA	147.5 nm	NA	−20.4 mW	671 nm 300 mW cm^{-2}	8 min	100 μg mL^{-1}	4T1	77
O_2@UiO-66 @ICG@RBC	ICG	RBC	1404 cm^2 g^{-1}	64.7 nm	91.2 nm	−11.0 mV	808 nm 0.06 W cm^{-2}	5 min	200 μg mL^{-1}	MCF-7	68
MB@THA-NMOF76 @cRGD	MB	cRGD	244.5 m^2 g^{-1}	0.6 nm	89 nm	25.6 mV	808 nm 0.5 W cm^{-2}	5 min	20 μg mL^{-1}	A549 HeLa	80
Ce6@MOF-199 TPAAQ@MOF-199	Ce6 TPAAQ	F-127	215.2 m^2 g^{-1} 180.3 m^2 g^{-1}	0.7–2.5 nm	NA		400 – 700 nm 0.5 W cm^{-2}	5 min	10 μg mL^{-1}	HepG2 NIH-3T3	24
Ce6@CMOF Ce6@RMOF	Ce6	F-127	NA	>100 nm	NA	∼20 mV	660 nm 100 mW cm^{-2}	10 min	20 μM	4T1	79
L-Arg@PCN @Mem	TCPP	Mem	NA	NA	NA	NA	660 nm 30 mW cm^{-2}	8 min	40 mg L^{-1} (TCPP) 50 mg L^{-1} (L-Arg)	4T1 CT26	85
RC@TFC	Ce6	TA RAP CAT	NA	160 nm	NA	NA	635 nm 0.75 W cm^{-2}	5 min	5 μg mL^{-1}	MDA-MB-231	31
PDA-MB-CAT-ZIF-8 (PMCZ)	MB	PDA CAT	NA	NA	3.4 Å	13.2 mV	660 nm 100 mW cm^{-2}	3 min	50 μg mL^{-1}	HeLa	86
CPC@MOF	Ce6-labelled CaB	Cam, HOOC-PEG-FA	NA	2.8 nm	95 nm	−17.7 mV	660 nm 200 mW cm^{-2}	5 min	1.6 μM	HeLa	9
FZIF-8/DOX-PD-FA	Ce6	Si-Gd NPs DOX HOOC-PDMAEMA-SH PEG-FA	845.8 m^2 g^{-1}	70 nm	NA	5.0 mV	630 nm 300 mW cm^{-2}	5 min	1 mg mL^{-1}	MCF-7 A549	84
CM-MMNP	TCPP	MnO2 PEG-600 Cell membrane	NA	NA	160 nm	−63.41 mV	409 nm 1.5 W cm^{-2}	5 min	3.2 μg mL^{-1}	HeLa HepG2 3T3	87
Ir@MOF/P NP	Biscyclometalated iridium(III)	BP PDM PG	NA	NA	320.1 nm	NA	10 mW cm^{-2}	30 min	20 μg mL^{-1}	HeLa	6
Fe-soc-MOF@PEG-NH_2-ICG (FPINS)	ICG	Oleic acid PEG	678.46 m^2 g^{-1}	0.57 nm ∼100 nm	NA	−8.7 mV	808 nm 0.88 W cm^{-2}	300 s	100 μg mL^{-1}	HeLa	78

Key: PS-photosensitizer, others: other constituents, BET: surface area, zeta ζ: surface potential, λ: wavelength, time: time of exposure, [PS]: concentration of PS.

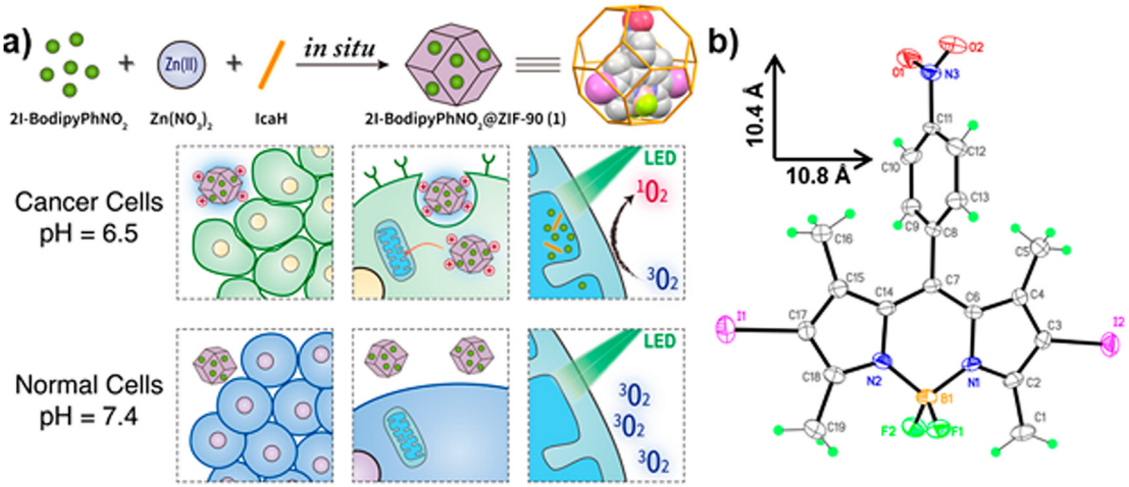

Fig. 6 Schematic representation of the (a) synthesis of 2I-BodipyPhNO$_2$ and the effect of pH-driven selective uptake toward cancer and normal cells. (b) Perspective view of 2I-BodipyPhNO$_2$ (reproduced with permission from ref. 73. Copyright 2018, American Chemical Society).

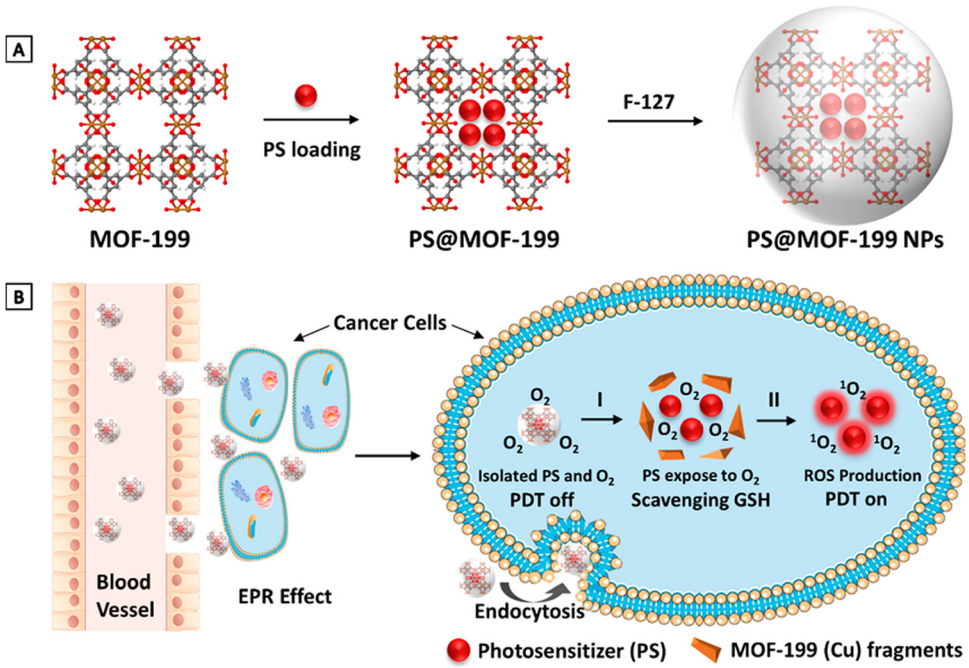

Fig. 7 (A) Synthesis of PS@MOF-199 NPs. (B) Quench and trigger of photosensitization from PS@MOF-199 NPs in the tumor microenvironment (reproduced with permission from ref. 24. Copyright 2019, American Chemical Society).

The rigid crystal matrix of ZIF-8 hindered the movement of molecules of the complex, which enhanced the implemented room temperature phosphorescence (RTP) properties. The host–guest interactions also influenced the intensity, quantum yield, and extended decay period of the nanoprobe. An exceptional linear relationship was established between the phosphorescence decay lifetime, intensity and oxygen concentration.[75]

Ir@MOF/PNP consists of poly[(2-acryloyl)ethyl(*p*-boronic-acidpinacolesterbenzyl)-diethylammoniumbromide](BP), poly-[2-(5,5-dimethyl-1,3-dioxan-2-yloxy)ethylacrylate] (PDM) and cyclo-dextrin-functional poly(glycerol methacrylate) (PG) segment (BP-PDM-PG). This biscyclometalated iridium(III) complex was applied for PDT due to its prolonged triplet excited state in the NIR under visible light and high oxygen sensitivity, which facilitates its low oxygen tension. The dual-responsive polycationic segment coated on MOF was subjected to charge conversion from positively to negatively charged ROS, which weakened the electrostatic interaction between the MOF and polymers, but benefited the efficient release of Ir(III). BP influenced the ROS-responsive segment with charge reversal properties. The release of MOF was accelerated by pH and the ROS-responsiveness of BP-PDM-PG. The advantages of the MOF include good biocompatibility in the dark,

a large amount of noxious ROS under daylight irradiation for a short time, significant anti-cancer efficiency, and apparent endo/lysosome escape at minimal concentration.[6]

Metal organic frameworks employed as carriers with multifunctional theranostic platforms for PDT

The structures of multifunctional MOFs efficiently utilize the metal ions and the organic ligands to exert their full therapeutic function as a carrier-free biodegradable system. Also they can serve as stimuli-responsive nanocarriers in physiological environments. The tumor targeting ability of PS is enhanced by the morphology, particle size and surface modulation.[2,37]

The large surface area of PCN-224 NMOF is responsible for the high loading capacity of doxorubicin (DOX) through physical adsorption, facilitating the transfer of drugs to cancerous cells and PDT. The functionalized variant HA-PCN loaded with DOX showed high colloidal stability. As a gate keeper, HA (hyaluronic acid) blocked the entrance of the pores in order to prevent premature drug release. The HA-DOX-PCN system ensured specificity in the targeting of cancer cells, and DOX was triggered by the stimulation of the enzyme HAdase.[68] DOX@PCN-224-DNA can monitor and focus on A549 cells with drug delivery and photodynamic effect, as seen in Fig. 8.[44] The accommodation of hyaluronic acid (HA) in MOFs loaded with drugs can result in an enzyme-responsive MOF, which can stimulate drug release and selective accumulation of drug carriers in overexpressed cancer cells. HA served as an external covering on the surface of HA-Dox-PCN-224 *via* multivalent coordination. It prevents premature release and sustains the presence of drug molecules inside the pores by blocking the entry through poly-covalent coordination bonds and electrostatic interactions, as depicted in Fig. 9.[68] The covalently functionalized hybrid zirconium-based UiO-66-N_3 MOF using azide click chemistry produced DOX/UiO-66-PEG-F3. The MOF was responsible for the pH-responsive release of DOX. The presence of the F3 peptide enhanced the targeting of cancer cells, which led to stronger accumulation in the cells. Post-modification was employed to improve the structural stability of UiO-66-N_3.[76]

A multifunctional theranostic platform for promoting PDT imparts synergistic therapy that inhibits the accumulation of NPs at the local tumor and the occurrence of tumor growth with insignificant side effects. In PCN-CuS-FA-ICG nanocomposite, PCN-222 served as a carrier for loading PS, which was instrumental to the production of a large amount of singlet oxygen and served also as a self-quencher. Surface modification of PCN with FA serves as a target folate receptor. CuS NPs anchored on the MOF imparted strong photothermal abilities and enhancement of PDT.[77] The reaction-based catalytic cascade in P@Pt@P-Au-FA, as shown in Fig. 10, was responsible for its distinct compositions, enhanced physiological stability, effective tumor accumulation performance, significant relief toward intra-tumoral H_2O_2, enhanced PDT, and glucose depletion-induced synergistic starving-like abilities *in vivo*. Here, the Pt NPs were embedded with Au NPs for catalase and glucose oxidase mimicking. The abundant PCN channels in the shells of MOF were utilized for confinement and stabilization of Au NPs. Pt NPs catalysed the intra-tumoral decomposition of peroxide to evolve sufficient oxygen effective for tumor hypoxia attenuation. Au NP depletes intra-tumoral glucose and the process can be fast-tracked by the production of oxygen, which reduces the nutrient supply and energy. This leads to a boost in the therapy, and the prevention of tumor recurrence and metastasis. FA was employed for additional linkage to improve the physiological stability through the introduced coordination between the carboxyl groups and Zr clusters.[78] The physiochemical properties and structural diversity of Fe-soc-MOF@PEG-NH_2-ICG (FPINs) were responsible for their utilization as nanovehicles for imaging and drug molecules. Fe-Soc-MOF served as a carrier to enhance the stability of ICG, whereas its degradation in aqueous solution was hindered by the stability imparted by ICG. Also, the presence of ICG conjugated to

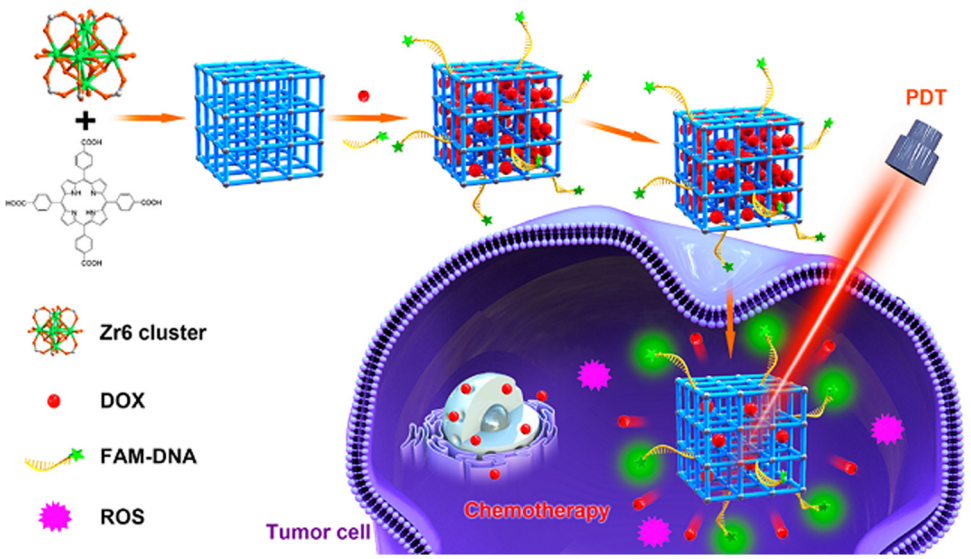

Fig. 8 Graphic illustration of DNA-functionalized PCN-224 for target drug delivery and PDT (reproduced with permission from ref. 44. Copyright 2019, American Chemical Society).

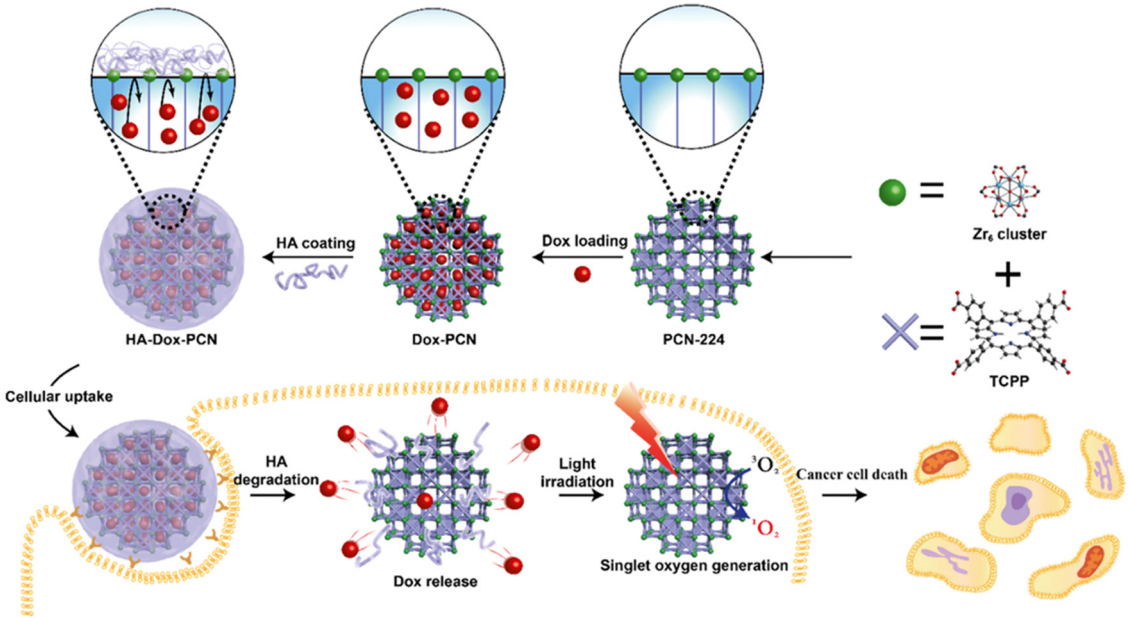

Fig. 9 Synthesis of the MOF x biopolymer nanosystem for combined chemotherapy and PDT therapy (reproduced with permission from ref. 68. Copyright 2019 American Chemical Society).

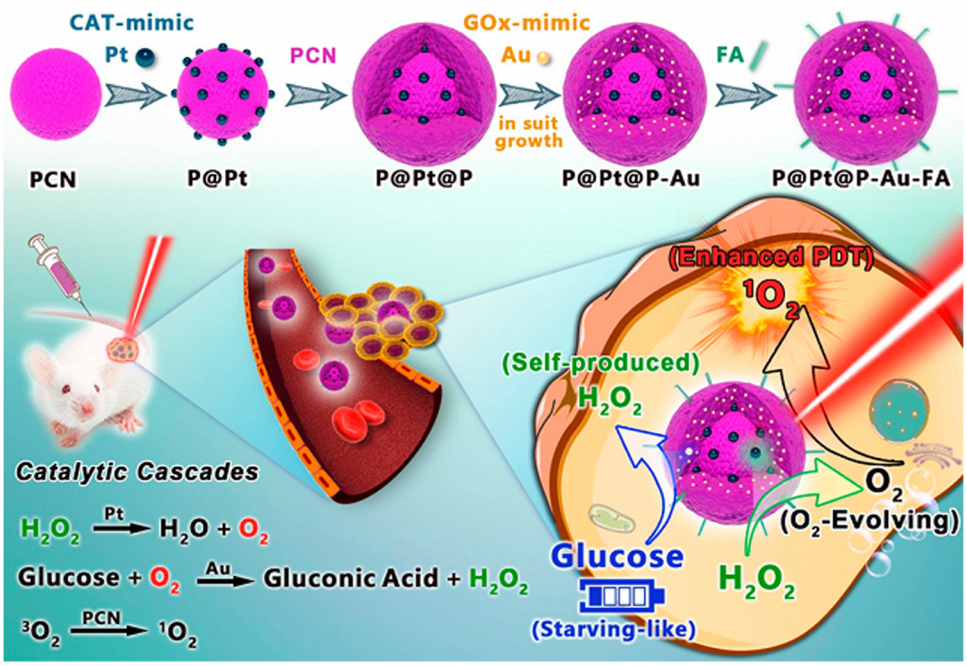

Fig. 10 Graphic illustration of nanozymes-engineered porphyrin MOFs (PCN) for catalytic cascade-enhanced synergistic cancer therapy (reproduced with permission from ref. 77. Copyright 2019 American Chemical Society).

the surface-modified Fe-Soc-MOF presented a multifunctional theranostic platform. Functionalization of the NMOF platform with PEG enhanced its dispersibility in water. The nanoplatform is promising for cancer diagnosis and treatment due to its excellent therapeutic effect, good biocompatibility and low toxicity.[79] The multifunctional Ce6@RMOF nanovehicle with disulfide containing imidazole and zinc exhibited broad sensitivity to singlet oxygen, GSH and pH, courtesy of the imidazole and disulfide groups. The MOF nanocarrier possessed a large void space due to high cargo loading. The organic ligand controlled the MOF nanocarrier, while the GSH trigger activated the already tailored nanocarrier. In addition, the sensitivity of MOF to GSH is reflected by the thiol–disulfide reaction, which is strengthened by the continuous increase in particle size upon incubation

with GSH in aqueous medium. The coating of the MOF cores with amphiphilic Pluronic F127 was responsible for the dispersibility and stearic stabilization of the MOF nanocarrier in aqueous medium. Also, the size of the nanocarrier was increased by encapsulation with Ce6. The presence of disulphide, along with ionization of the imidazole at low pH, promoted improved cargo release in response to GSH supplementation and breakdown of the MOF. Oxidation of the imidazole facilitated cargo liberation by production of photo-triggered singlet oxygen. Ce6@RMOF is an all active MOF that is activatable and adaptable and a MOF-based multifunctional nanoprobe that possesses dual therapeutic functionality for target-controlled PDT and chemotherapy effects.[80] The synthetic ease, good biocompatibility, higher loading efficiency of the Ce6-peptide and drug molecule were features of the multifunctional probe. The MOF functionalized with the amino group (NH_2) served as the vehicle, site of modification, and quencher. Cathepsin B(CaB)-activatable fluorescence imaging was due to the presence of the camptothecine drug and chlorin e6 (Ce6) as a photosensitizer. Non-covalent encapsulation of the camptothecine drug bound with target element – folic acid and CaB substrate peptide, while Ce6 served as a signal switch and for the recognition of the moiety. This integrated platform causes a reduction in side effects, retardation of multidrug resistance of chemotherapeutics, and overcomes the low efficiency of PDT in hypoxia cells.[9]

O_2@UiO-66@ICG@RBC achieved passive tumor targeting *in vivo*, long circulation and self-sufficient O_2, co-delivery of O_2 and photosensitizers, which was effective for the treatment against hypoxia tumors without adverse effects to healthy tissues. UiO-66 was employed as a carrier for oxygen storage due to its biocompatibility and high absorption capacity. The as-prepared NPs encapsulated inside RBC membranes provided a biomimetic oxygen-evolving PDT nanoplatform. The anchoring of ICG on the MOF occurred through coordination of Zr6 clusters with sulphonic acid groups. ICG produces primary singlet oxygen that depletes RBC membranes and triggers laser radiation for the burst release of O_2 from UiO-66.[69] MB@THA-NMOF-76@cRGD NP was postsynthetically modified with β-diketonate, a two photon-absorbing (TPA) ligand, functionalized by methylene blue (MB). The PS was assembled in its pores, along with cyclic peptide targeted on the surface of the MOF. The NMOF achieved highly efficient near-infrared (NIR) triggered and targeted PDT. Coordination of Eu^{3+} with NMOF-76 functionalized with HTHA imparted TPL with emission properties on THA-NMOF for the absorption of light at 808 nm. The NIR-excited PDT was accomplished *via* LRET process, in which Eu^{3+} emitted light at 615 nm and MB was excited in the NMOF pores. A high tissue-penetrable TPA-PDT effect was achievable due to the transfer of luminescence resonance energy between the photosensitizer (MB), acceptor and the NMOF donor. The NMOF possessed effective PDT toward cancer cells and enhanced cellular uptake for *in vitro* studies. Hence, they were effective and safe for the treatment of neoplasms as potential drug delivery platforms and PDT agents.[81]

The copper porphyrin-based MOF composite – F68-DOX@CuTPyP was employed as a vehicle for the delivery of DOX. Meanwhile, their residence time increased in tissues and endocytosis was promoted in cells. The overall effect leads to inhibition of viable cancer cells, tumor growth, and combating drug-resistant tumors.[82] MOF can serve dual purposes as PS and vehicles. The loading of MOF with inhibitors can cause a synergistic effect in the application of MOF for PDT, along with increased efficacy, sensitivity and specificity. In PCN-222 loaded with piperlongumine (PL) and thioredoxin reductase (TrxR), the release of PL induced imbalance of redox homeostasis, which depressed TrxR, hindered the ROS pathway for elimination, and enhanced the sensitivity of the cancer cells to damage.[83] Zeng *et al.* (2021) studied the hybrid MIL-88B(Fe)@ZIF-8, which was employed as cargo for loading DOX, manganese oxide nanoparticles and folic acid. The MOF's multifunctional platform integrated targeting, imaging and chemotherapeutic functionality for smart therapy with high efficiency and specificity.[84]

A self-assembled multifunctional MOF nanoplatform (FZIF-8/DOX-PD-FA) integrated Si-Gd NPs (Gd-doped silicon nanoparticles), Ce6, DOX (doxorubicin), ZIF-8 (zeolitic imidazolate framework-8), HOOC-PDMAEMA-SH (poly(2-(diethylamino) ethylmethacrylate)) polymers and MaL-PEG-FA (folic acid poly-(ethylene glycol)-maleimide), as illustrated in Fig. 11. The entrapment of Si-Gd NPs and Ce6 was responsible for magnetic resonance and fluorescence dual-modal imaging, respectively. DOX was loaded into the porous structure of FZIF-8/DOX-PD-FA for chemotherapy, while Ce6 could be excited by NIR for PDT. In addition to its biocompatible and tumor targeting properties, the nanocomposite MOF avoided leakage of DOX with specific control as a result of the pH responsiveness of HOOC-PDMAEME-SH and target modification of NPs on the surface by PEG-FA. The NPs enhanced the therapeutic effects. The MOF platform also integrated PDT with chemotherapy for improved cancer treatment.[85]

The biomimetic and multifunctional L-Arg@PCN@Mem comprising PCN-224 and L-Arg coated with a cancer membrane possesses synergistic therapy based on gaseous nitric oxide and sensitive PDT. Here, PCN-224 served as a delivery vehicle loaded with L-Arg, which causes increased loading efficiency, avoids self-quenching, and ensures facile diffusion of singlet oxygen. Meanwhile, L-Arg serves as a natural nitric donor, which can be transformed through oxidation to NO. A dual function role performed by the light-responsive ROS in L-Arg@PCN@Mem was effective for PDT, and the gas therapy-involved mortality of cells and production of nitric gas. The efficacy of PDT in hypoxic tumors was enhanced by the transformation of ROS to NO, which was due to the capacity of NO to diffuse freely at the hypoxic tumor site. The MOF was coated with a cell membrane to improve tumor targeting. Also, the excellent homologous biotargeting role arose from encapsulation of the cancer cell membrane. Altogether, this improved tumor treatment resulted from the extended circulation time that hindered metabolic clearance, selective accumulation, and increased retention time at the tumor site with negligible side effects.[86]

The contribution of RC@TFC NPs was significant in the amplification of the therapeutic effects of PDT, removal of obstacles in cancer treatment, and proffered a universal synthetic solution. The construction of a core–shell nano RC@TFC NPs acted as an obstruction to the effectiveness of photodynamic

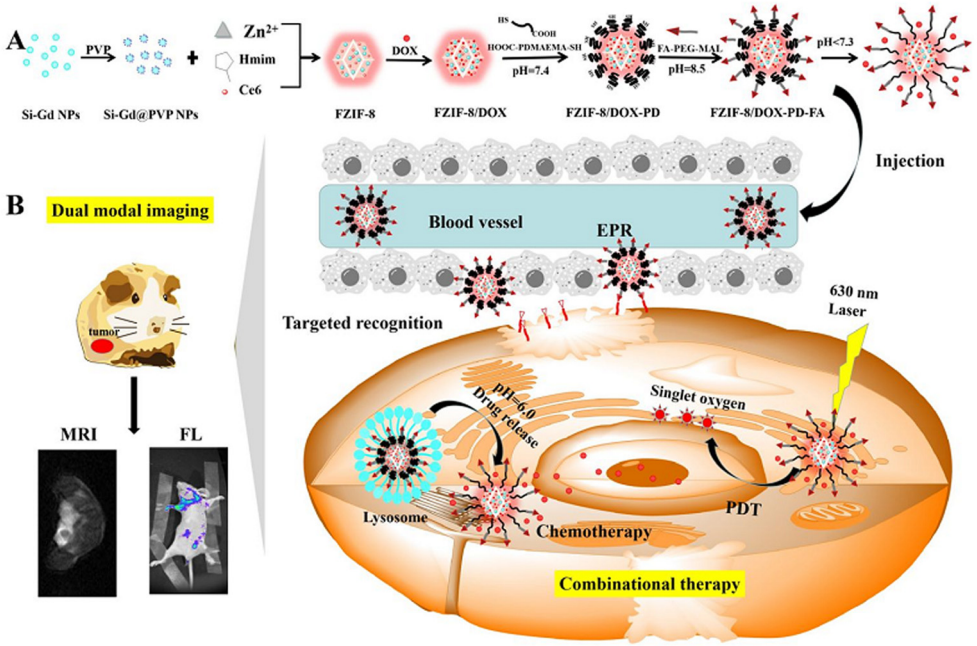

Fig. 11 Graphic representation of (A) the synthetic route of pH-responsive FZIF-8/DOX-PD-FA. (B) Fluorescence and magnetic resonance dual-modal imaging-guided chemo/photodynamic combinational cancer therapy (reproduced with permission from ref. 85. Copyright 2019, American Chemical Society).

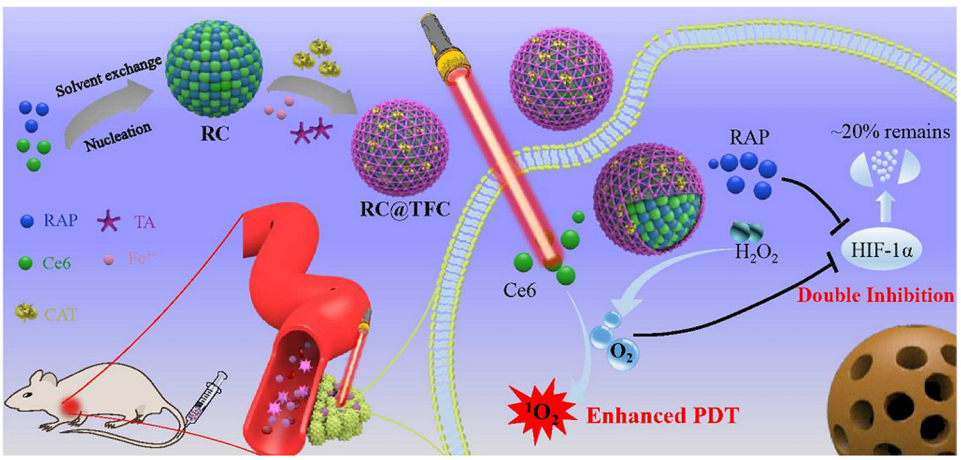

Fig. 12 Schematic representation of core–shell nano RC@TFC constructed for synergistic PDT therapy of cancer treatment (reproduced with permission from ref. 88. Copyright 2019 American Chemical Society).

therapy of the tumor, which reversed tumor hypoxia through alleviation and overcame restriction of PDT *via* suppression of the HIF-1α expression. The synthetic product comprised a hydrophobic photosensitizer (Ce6), rapamycin (RAP) and catalase in layer-by-layer coating of MOFs. This resulted in high co-loading and excellent colloidal capacity of Ce6, RAP and CAT. The hydrophobic Ce6 PS and RAP formed a carrier-free and dual drug nano-core coated with a layer of MOF to load the catalase. Fig. 12 shows the schematic representation of PDT for the multifunctional core–shell. In the MOF system, CAT supplied the oxygen, which catalyzed the decomposition of the tumor-abundant hydrogen peroxide and oxygen. RC@TFC NPs, under light irradiation, achieves dual function towards tumor cells through promotion of self-supplied oxygen and sustained release of RAP for regulation of HIF-1α. The features of the MOF nanosystem also include passive accumulation into the tumor, *in situ* production of oxygen, inhibition of HIF-1α and exhibition of a strong PDT effect towards extreme tumor hypoxia.[31] A multifunctional intelligent ZIF-8-gated polydopamine nanoparticle vehicle was designed for the selective release of PS, and continuous generation of oxygen to promote cancer therapy. The treatment improved the combinatorial efficiency that promoted efficient PDT, but ameliorated tumor hypoxic conditions with the CAT-mediated independent oxygen production. Encapsulation of

methylene blue PS and catalase caused an increase in efficiency of the MOF. The MOF NP possessed high biocompatibility with specific tumor features, and NIR absorption alongside evolution of oxygen was administered for the simultaneous transport of PS and catalase (CAT) in the tumor cells. The MOF NP carrier facilitated the concurrent effective delivery of functional payloads, and successive acidic pH tumor-stimulated drug release.[87]

MnO_2 nanosheets used as PS carriers exhibited electrostatic interaction and Mn–N coordinate bonds, which are responsible for the strong adsorption ability of PS to endocytose in intracellular PDT. It had good biocompatibility because Mn is nontoxic in physiological metabolism.[2] The smart nanostructure of the cell membrane-coated porphyrin MOF is composed of the MnO_2 nanosheet-coated MOF core and the cancer cell membrane shell (CM-MMNPs). The core structure is a porphyrin-based MOF coated with a thin layer of the MnO_2 nanosheet (MMNPs), as shown in Fig. 13. The O_2^--mediated singlet oxygen was enhanced by the production of O_2 from the MnO_2 layer, which displayed H^+ and H_2O_2 receptiveness in acidic solutions. Effective etching of the MnO_2 layer, after endocytosis under laser illumination, led to fluorescence recovery and enhanced oxygen generation that favoured the dual mode imaging and efficient PDT towards cancer cells, as illustrated in Fig. 13. The cell membranes in CM-MMNPs impart significant stability of the colloid in biological buffer and strong homologous cancer cell targeting ability.[89]

The A-NUiO@DCDA@ZIF-Cu multifunctional platform for PDT was prepared from UiO-66, Cu doped ZIF-8, and aggregation-induced emission active luminogens (AIEgens). UiO-66 modified with dodecanoic acid (DCDA) was used to load the AIEgens to enhance its fluorescence emission because of its robust crystallinity, chemical stability, loading capacity and ease of modification. The Cu-doped ZIF-8 was used to encapsulate A-NUiO (AIEgen loaded UiO-66) to provide a core shell material due to its tunable shape, size and TME (tumor microenvironment)-stimuli responsive degradation ability. A-NUiO@DCDA@ZIF-Cu exhibits minimal non-specific toxicity with improved therapeutic activity, good ability to deplete GSH, amplify tumor oxidative stress, enhance tumor accumulation and retain AIEgens.[19]

The versatility of conventional MOF was enhanced using mixed-ligand MOF with adjustable ligand ratios that multiplied its properties. TCPP and Mn-TCPP were utilized as mixed ligands connected to zirconium nodes for building the framework, which was loaded with 10-hydroxycamptothecin (HCPT) and modified with hyaluronic acid (HA) *via* the disulfide bond. The use of both TCPP and Mn-TCPP achieved high loading, surface modification with HA-enhanced PDT, and tumor-targeted redox-responsive drug release.[90]

Upconversion nanoparticles (UCNP) integrated with metal organic frameworks employed in photodynamic therapy

The possibility of UCNP to convert low energy photons with long wavelength into high energy emissions with short wavelength is responsible for their utilization in PDT.[8] PS integrated with UCNP results in efficient generation of ROS without compromising its efficacy at deeper penetration.[29] UCNP@MOF consists of UCNP and MOF applied in the PDT treatment of cancer.[1] UCNP are also promising carriers for anticancer drugs or PS in PDT.[2] Table 3 is a summary of the constituents of UCNPs and the conditions for their application.

A core shell heterostructure of UCNP@MOF was employed for combined therapy against hypoxic tumors. The NIR light generated the release of ROS due to efficient energy transfer between UNCP and the MOF that leads to increased efficacy. Loading of the pores of the MOF with TPZ (Tirapazamine) enabled effective combinational therapy for NIR-triggered PDT and hypoxia-activated chemotherapy. The combination of the

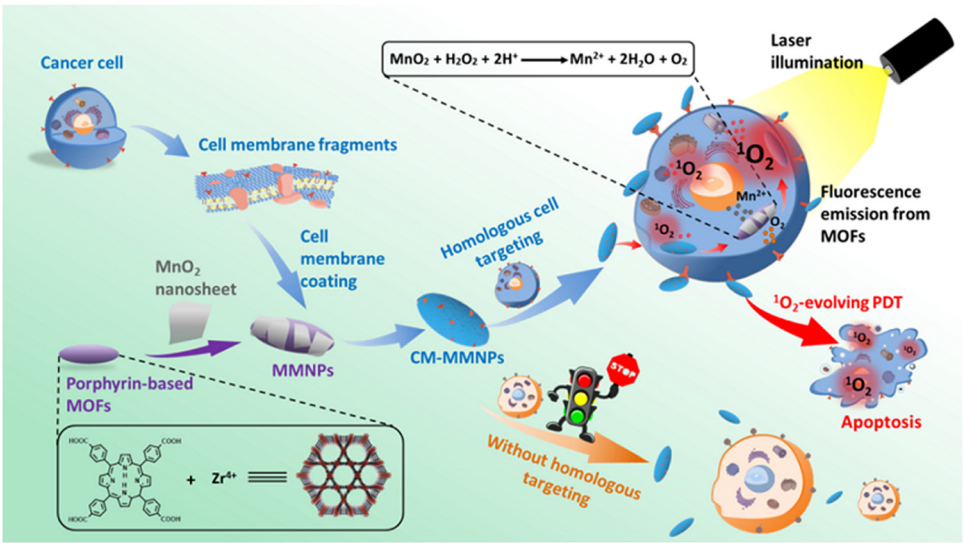

Fig. 13 Graphic representation of CM-MMNPs applied in cancer treatment for homologous targeting and PDT (reproduced with permission from ref. 89. Copyright 2019 American Chemical Society).

Table 3 Properties of UCNPs applied for PDT

MOF	PS	Others	BET	Pore size	Diameter	Zeta ζ	λ and intensity	Time	[PS]	Cells type	Ref.
UCNPs-g-C_3N_4-CDs@ ZIF-8	g-C_3N_4 CDs	Oleic acid PEI	769 cm^2 g^{-1}	NA	150 nm	NA	980 nm 0.5 W cm^{-2}	5 min	1 mg mL^{-1}	HeLa L929	29
UC@mSiO_2-RB@ZIF-O_2-DOX-PEGFA (URODF)	RB	mSiO_2 ZIF-90 DOX PEG FA	556.2 m^2 g^{-1}	184 nm	NA	NA	808 nm 0.5 mW cm^{-2}	10 min	100 μg mL^{-1}	4T1 HeLa	91
UMOF-TiO_2	TCPP	TiO_2 PVP	356.149 m^2 g^{-1}	NA	120 nm	−20	980 nm 0.72 W cm^{-2}	5 min	1 mg mL^{-1}	MCF-7	90
PVP-UCNP@ MOF CA-UCNP@ MOF		TPZ PVP CA		38–65 nm	~46 × 8 nm	13.8 mV −4.7 mV	980 nm 1.2 W cm^{-2}	10 min	25 μg mL^{-1}	CT26	89

Key: PS-photosensitizer, others: other constituents, BET: surface area, zeta ζ: surface potential, λ: wavelength, time: time of exposure, [PS]: concentration of PS.

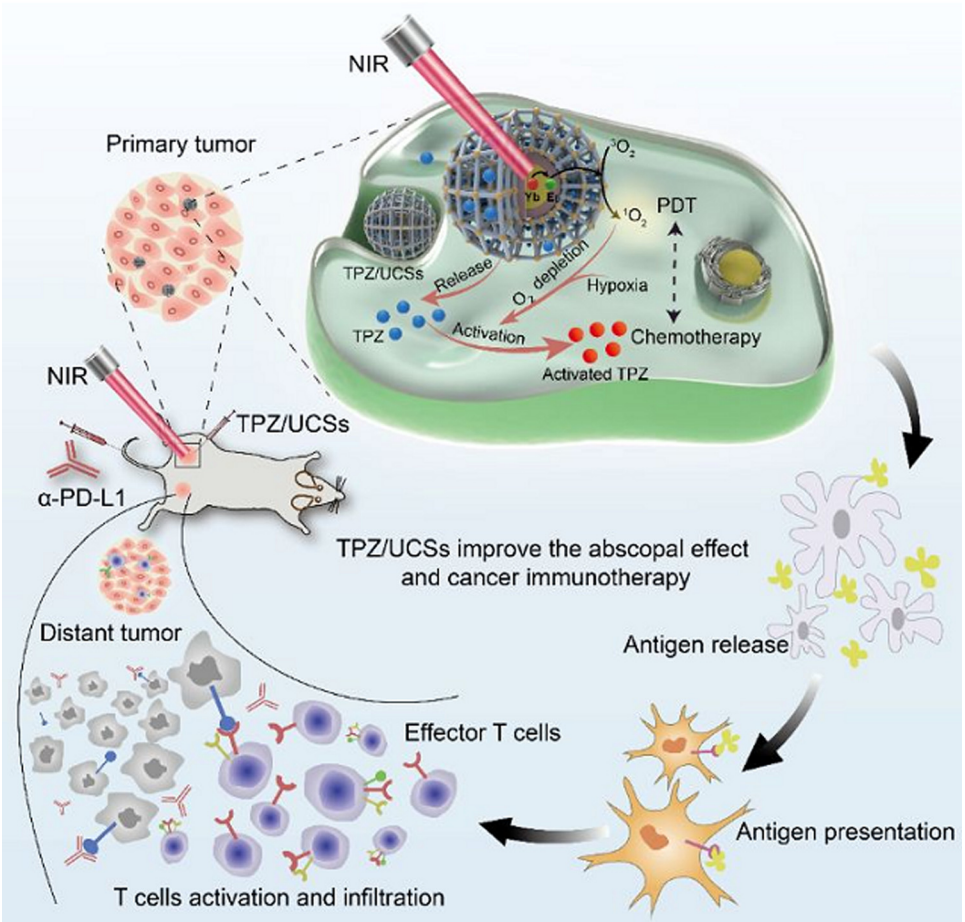

Fig. 14 Graphic representation of the combined application of engineered upconverted TPZ/UCS for chemotherapy with immunotherapy tumor treatment (reproduced with permission from ref. 91. Copyright 2020 American Chemical Society).

chemo and PDT stimulated efficient anti-tumor immunity, including integrated checkpoint blockade therapy for inhibition of tumors at distant sites. The illustration is depicted in Fig. 14.[91] The incorporation of UCNPs, TCPP-MOF and TiO_2 into a nanosystem, as illustrated in Fig. 15 below, produced a porphyrin-based MOF (UMOF-TiO_2) with deep penetration and effective multi-modal PDT performance of the photosensitive agent. The UMOF-TiO_2 nanocomposite-based carrier exhibited features, including increased stability, excellent biocompatibility, and water dispersibility. The nanoplatform is built by covering small TiO_2 NPs on a heterodimer made of UCNP and MOF. UCNP stimulates photochemical reactions of TiO_2

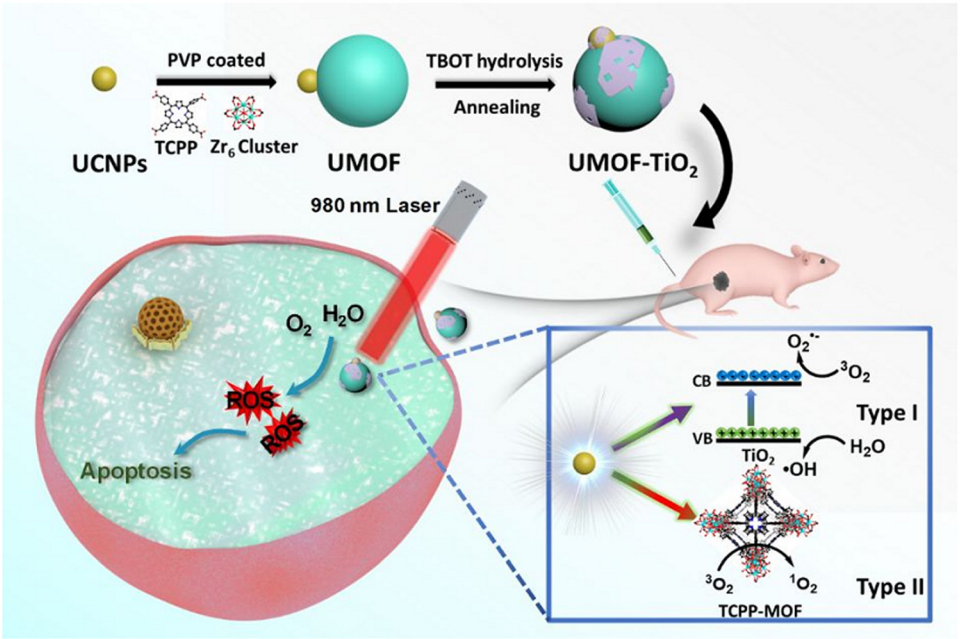

Fig. 15 Graphic illustration of the synthesis and PDT application of UMOF-TiO_2 (reproduced with permission from ref. 92. Copyright 2020 American Chemical Society).

and the porphyrin-based MOF to achieve PDT. The stimulation *via* laser irradiation in *in vivo* and *in vitro* experiments produced extremely cytotoxic ROS, leading to cancer cell apoptosis with minimal photo-damage and deep biological tissue penetration.[92]

UC@mSiO_2-RB@ZIF-O2-DOX-PEGFA (URDOF) is a multifunctional nanodrug carrier with dual function, PDT enhanced by oxygen and pH responsive chemotherapy. The upconversion/magnetic resonance imaging matrix and motivator for PS in PDT employed $NaYF_4$:Yb/Er@$NaYbF_4$:Nd@$NaGdF_4$ nanoparticles (UC). The carrier for rose bengal (RB) PS was mesoporous silica shell (mSiO_2), while the UCNP core shell was responsible for activation of RB in mSiO_2. The external coating of mSiO_2 by ZIF-90 served as an oxygen reservoir in the tumor microenvironment for quick oxygen release and tumor hypoxia alleviation for PDT enhancement. The improved synergetic therapy on the nanoparticle surface was due to covalent conjugation of DOX (doxorubicin) and NH_2-poly(ethylene glycol) modified with folic acid (PEGFA).[93]

UCNPs-g-C_3N_4-CDs@ZIF-8, an integrated, dual PDT model, was prepared by attachment of core–shell structured UCNPs, NaGdF4:Yb and Tm@NaGdF4 on graphitic-phase carbon nitride (g-C_3N) nanosheets, followed by assembly of ZIF-8 MOF by *in situ* growth process. The efficacy of ZIF-8 remained intact, and the successive initiation of g-C_3N_4 and carbon dots was allowed. The UCNPs converted low energy NIR and deep-penetration light to higher energy UV emission that corresponded to the range required for the production of ROS. The integrated hybrid combined maximum energy utilization with non-toxicity and excellent biocompatibility to achieve enhanced anti-proliferation efficiency. The system efficiently transported the energy photon by deep penetration to activate g-C_3N_4 and CDs, produced ROS rapidly and killed cancerous cells efficiently. The presence of ZIF-8 shells stored ample oxygen and water for PDT effect, but hindered environmental influence of the fluorescence intensity, which was superior to the mesoporous silica. The composite was highly efficient for both *in vivo* and *in vitro* anti-proliferation of cancer cells.[29]

Summary and conclusion

Several outcomes have evolved and emerged, which reveals that the limitation of the existing therapeutic methods in PDT can be overcome by the application of MOFs. The strengths of MOFs employed as PS include biocompatibility, bioavailability, effective clearance, target delivery, response and minimal toxicity. This review summarizes the importance of the design strategies of MOF in PDT, which includes the backbone, its metal centers, and the various SBU utilized to achieve an efficient and effective system. It also highlights the significance of the use of MOFs as PS, vehicles for transport of PS and other materials that enhances the treatment of cancer with PDT. Furthermore, recent progress in the use MOFs with various multitheranostic platforms was also discussed. The importance of pristine MOFs as good inhibitors and suppressors with short retention times in the system and simple clearance mechanisms in PDT was reported. Their functionalized counterparts provide platforms that integrate multiple functionalities, overcoming hydrophobicity and ensuring stability, long retention times and target delivery. It was observed that MOFs which function as PS have smaller pore diameters when compared to their functionalized counter parts (Table 1). However, the linkers can be tuned to control the pore size to ensure the suitability of the MOFs to be used as carriers. MOF employed as PS used photosensitive building blocks, while those employed as carriers used existing

MOF structure as vehicles (Table 2). UCNPs were observed to introduce tuning of the MOF structure with a core shell to ensure deeper penetration of photons.

The following accomplishments in the recent advances of MOFs, which employed active metal ion/clusters, PS integrated into scaffold or PS carried by MOFs in PDT are as follows:

(i) PSs integrated in the MOF framework were well isolated in the framework to avoid agglomeration and self-quenching of the excited states.

(ii) MOF molecules decomposed into small molecules and ions, which can be effectively cleared from the body.

(iii) Minimal long-term toxicity concerns and low, nontoxic retention in organs can be achieved.

(iv) The dissemblance of well-ordered hydrophobic PS into MOF scaffolds addressed the issues of solubility and bioavailability of hydrophobic PS.

(v) High dispersion of PS in the MOF matrix effectively hinders aggregation caused by quenching.

(vi) MOFs ensured the efficient delivery of PS and the restriction of complex molecules motion implements RTP properties.

(vii) PS loaded in MOFs with active redox metal centers facilitated activatable photosensitization, cancer cell-specific PDT with improved efficiency.

(viii) MOFs with functionalized backbones and specific building blocks add different functionalities to nanocarriers, which make them efficient and stimuli-responsive in physiological environments.

Future outlook

These studies have shown that MOFs are promising materials for PDT. However, there are potentials for the future development of MOFs in the following areas. The clinical applications of MOFs in PDT for the treatment of cancer should be further explored. In addition, the design of multifunctional MOFs assembled using multitudinous biomolecules that can integrate selective target-imaging of cancer cells, feedback and stepwise therapy will advance its clinical applications. The use of biologically active materials as linkers and functional materials, along with biological metals, for the design of the MOFs is a promising approach. Smart MOFs that are intelligent in nature with multimodal functions, along with the ability to respond based on the cellular environment, and can deliver efficiently with specificity to the target also have potentials in PDT. The utilization of photoswitchable MOFs tailored with the ability to trigger PDT treatment that can serve as multifunctional stimuli-responsive materials should be considered. MOFs can also be designed for application in complex biological media with a simplified approach without collapse in the presence of phosphate species and for immature release before arrival at the target location. The fabrication of MOFs with the capacity to bear an inner light source, which is not dependent on an external source, and near-infrared lights that allows for deeper penetration will solve the issue of poor light penetration. Also, incorporation of intelligent gatekeepers that will stimulate the release of therapeutic agents, facilitate efficient delivery of PS and TA, and ameliorate tumor hypoxic conditions also holds the future in PDT.

Abbreviations

BODIPY	Borondipyrromethene
BP	Poly[(2-acryloyl)ethyl-(*p*-boronic acid pinacol ester benzyl)-diethylammonium bromide]
CaB	Cathepsin B
Cam	Camptothecine
CAT	Catalase
Ce6	Chlorin e6
CM	Cell membrane
2D, 3D	2/3-Dimensional
DOX	Doxorubicin
EPR	Enhanced Permeation and Retention
FA	Folic acid
F127	Poloxamer
GSSG	Glutathione disulphide
GSH	Glutathione
H_2P	Tetrakis(4-aminophenyl)-21*H*,23*H*-porphine
HIF-1α	Hypoxia inducible factor-1α
HTHA	4,4,4-Trifluoro-1-(9-hexylcarbazol-3-yl)-1,3-butanedione
ICG	Indocyanine green
LRET	Luminescence resonance energy transfer
MB	Methylene blue
NIR	Near-infrared
NMOF	Nanoscale MOF
NP	Nanoparticles
PC	[(Pyr)4cyclen]
PG	Cyclodextrin-functional poly(glycerol methacrylate)
PDM	Poly[2-(5,5-dimethyl-1,3-dioxan-2yloxy)ethyl acrylate]
PEG	Polyethylene glycol
PL	Piperlongumine
PLL	Polylysine
PS	Photosensitizers
PVP	Polyvinylpyrrolidone
RAP	Rapamycin
RB	Rose bengal
RBC	Red blood cell
ROS	Reactive oxygen species
RTP	Room temperature phosphorescence
SQ	Squarine
TA	Tannic acid
TA	Targeting agent
TCPP	Tetrakis(4-carboxyphenyl)porphyrin
TEA	Triethylamine
TME	Tumor micro-environment
TPP	Triphenylphosphine
TPAAQ	2-(4-(Diphenylamino)phenyl)anthracene-9,10-dione
TPL	Two-photon luminescence

TPP-SH	5-(4-(*S*-Ethylthiol ester)thiocarbonylphenyl)-10,15,20-tris(4chlorophenyl)porphyrin
TPZ	Tirapazamine
ZIF-8	Zeolitic imidazolate framework

Data availability

This review article does not contain new data, software or code that have been generated by the authors. All of the data referenced in this paper are available in the original publications that are cited in the reference list.

Conflicts of interest

There are no conflicts to declare.

References

1 Q. Guan, Y. A. Li, W. Y. Li and Y. Bin Dong, Photodynamic Therapy Based on Nanoscale Metal–Organic Frameworks: From Material Design to Cancer Nanotherapeutics, *Chem. – Asian J.*, 2018, **13**, 3122–3149.
2 J. Chen, T. Fan, Z. Xie, Q. Zeng, P. Xue, T. Zheng, Y. Chen, X. Luo and H. Zhang, Advances in nanomaterials for photodynamic therapy applications: status and challenges, *Biomaterials*, 2020, **237**, 119827.
3 J. Liu, C. Zhang, T. W. Rees, L. Ke, L. Ji and H. Chao, Harnessing ruthenium(II) as photodynamic agents: encouraging advances in cancer therapy, *Coord. Chem. Rev.*, 2018, **363**, 17–28.
4 M. I. Khan, M. I. Hossain, M. K. Hossain, M. H. K. Rubel, K. M. Hossain, A. M. U. B. Mahfuz and M. I. Anik, Recent Progress in Nanostructured Smart Drug Delivery Systems for Cancer Therapy: A Review, *ACS Appl. Bio Mater.*, 2022, **5**, 971–1012.
5 L. Fang, Q. Hu, K. Jiang, X. Zhang, B. Li, Y. Cui, Y. Yang and G. Qian, An inner light integrated metal–organic framework photodynamic therapy system for effective elimination of deep-seated tumor cells, *J. Solid State Chem.*, 2019, **276**, 205–209.
6 Y. Zhang, H. Fu, S. Chen, B. Liu, W. Sun and H. Gao, Construction of an iridium(III)-complex-loaded MOF nanoplatform mediated with a dual-responsive polycationic polymer for photodynamic therapy and cell imaging, *Chem. Commun.*, 2020, **56**, 762–765.
7 L. Huang, S. Zhao, J. Wu, L. Yu, N. Singh, K. Yang, M. Lan, P. Wang and J. S. Kim, Photodynamic therapy for hypoxic tumors: advances and perspectives, *Coord. Chem. Rev.*, 2021, **438**, 213888.
8 T. C. Pham, V. N. Nguyen, Y. Choi, S. Lee and J. Yoon, Recent Strategies to Develop Innovative Photosensitizers for Enhanced Photodynamic Therapy, *Chem. Rev.*, 2021, **121**, 13454–13619.
9 J. Liu, L. Zhang, J. Lei, H. Shen and H. Ju, Multifunctional metal–organic framework nanoprobe for cathepsin B-activated cancer cell imaging and chemo-photodynamic therapy, *ACS Appl. Mater. Interfaces*, 2017, **9**, 2150–2158.
10 C. He, D. Liu and W. Lin, Nanomedicine Applications of Hybrid Nanomaterials Built from Metal–Ligand Coordination Bonds: Nanoscale Metal–Organic Frameworks and Nanoscale Coordination Polymers, *Chem. Rev.*, 2015, **115**, 11079–11108.
11 X. Zheng, L. Wang, M. Liu, P. Lei, F. Liu and Z. Xie, Nanoscale Mixed-Component Metal–Organic Frameworks with Photosensitizer Spatial-Arrangement-Dependent Photochemistry for Multimodal-Imaging-Guided Photothermal Therapy, *Chem. Mater.*, 2018, **30**, 6867–6876.
12 H. Wang, D. Yu, J. Fang, C. Cao, Z. Liu, J. Ren and X. Qu, Renal-Clearable Porphyrinic Metal–Organic Framework Nanodots for Enhanced Photodynamic Therapy, *ACS Nano*, 2019, **13**, 9206–9217.
13 M. Li, Y. Wang, H. Lin and F. Qu, Hollow CuS nanocube as nanocarrier for synergetic chemo/photothermal/photodynamic therapy, *Mater. Sci. Eng., C*, 2019, **96**, 591–598.
14 Y. Zheng, Z. Li, H. Chen and Y. Gao, *Nanoparticle-based drug delivery systems for controllable photodynamic cancer therapy*, Elsevier B.V., 2020, vol. 144.
15 D. Gao, Y. Gao, J. Shen and Q. Wang, Modified nanoscale metal organic framework-based nanoplatforms in photodynamic therapy and further applications, *Photodiagn. Photodyn. Ther.*, 2020, **32**, 102026.
16 D. Xu, Y. You, F. Zeng, Y. Wang, C. Liang, H. Feng and X. Ma, Disassembly of Hydrophobic Photosensitizer by Biodegradable Zeolitic Imidazolate Framework-8 for Photodynamic Cancer Therapy, *ACS Appl. Mater. Interfaces*, 2018, **10**, 15517–15523.
17 Z. Zhou, L. Zhang, Z. Zhang and Z. Liu, Advances in photosensitizer-related design for photodynamic therapy, *Asian J. Pharm. Sci.*, 2021, **16**, 668–686.
18 J. S. Oh, Y. You, K. C. Park, G. Gupta, D. K. Kang and C. Y. Lee, Toward an efficient photosensitizer for photodynamic therapy: incorporating BODIPY into porphyrinic nanoscale MOFs through the solvent-assisted ligand incorporation, *Dyes Pigm.*, 2019, **170**, 107576.
19 M. J. Dong, W. Li, Q. Xiang, Y. Tan, X. Xing, C. Wu, H. Dong and X. Zhang, Engineering Metal–Organic Framework Hybrid AIEgens with Tumor-Activated Accumulation and Emission for the Image-Guided GSH Depletion ROS Therapy, *ACS Appl. Mater. Interfaces*, 2022, **14**, 29599–29612.
20 J. Oyama, Á. C. Fernandes Herculano Ramos-Milaré, D. S. S. Lopes Lera-Nonose, V. Nesi-Reis, I. Galhardo Demarchi, S. M. Alessi Aristides, J. Juarez Vieira Teixeira, T. Gomes Verzignassi Silveira and M. V. Campana Lonardoni, Photodynamic therapy in wound healing in vivo: a systematic review, *Photodiagn. Photodyn. Ther.*, 2020, **30**, 101682.
21 K. Shanmugapriya and H. W. Kang, Engineering pharmaceutical nanocarriers for photodynamic therapy on wound healing: review, *Mater. Sci. Eng., C*, 2019, **105**, 110110.
22 M. Zhao, W. Zhang, M. Fan, Z. Xu, Y. Jiang, Z. Li, P. Zhai, X. Zhang, T. Chen, Y. Zhang, C. Yang, L. Li, G. Feng and G. Xu, AIEgen Photosensitizer-Loaded Silica Nanoparticles for Lysosomes-Targeting Photodynamic Therapy in Tumor, *ACS Appl. Nano Mater.*, 2024, **7**, 23504–23512.

23 J. J. Hu, Q. Lei and X. Z. Zhang, Recent advances in photonanomedicines for enhanced cancer photodynamic therapy, *Prog. Mater. Sci.*, 2020, **114**, 100685.
24 Y. Wang, W. Wu, J. Liu, P. N. Manghnani, F. Hu, D. Ma, C. Teh, B. Wang and B. Liu, Cancer-Cell-Activated Photodynamic Therapy Assisted by Cu(II)-Based Metal–Organic Framework, *ACS Nano*, 2019, **13**, 6879–6890.
25 S. S. Wan, Q. Cheng, X. Zeng and X. Z. Zhang, A Mn(III)-sealed metal–organic framework nanosystem for redox-unlocked tumor theranostics, *ACS Nano*, 2019, **13**, 6561–6571.
26 S. Wang, X. Wang, L. Yu and M. Sun, Progress and trends of photodynamic therapy: from traditional photosensitizers to AIE-based photosensitizers, *Photodiagn. Photodyn. Ther.*, 2021, **34**, 102254.
27 Z. Gao, F. Chen, Y. Li, Y. Zhang, K. Cheng, P. An and B. Sun, A small-sized and stable 2D metal–organic framework: a functional nanoplatform for effective photodynamic therapy, *Dalton Trans.*, 2019, **48**, 16861–16868.
28 M. Lismont, L. Dreesen and S. Wuttke, Metal–Organic Framework Nanoparticles in Photodynamic Therapy: Current Status and Perspectives, *Adv. Funct. Mater.*, 2017, **27**, 1–16.
29 D. Yang, G. Yang, S. Gai, F. He, C. Li and P. Yang, Multifunctional Theranostics for Dual-Modal Photodynamic Synergistic Therapy via Stepwise Water Splitting, *ACS Appl. Mater. Interfaces*, 2017, **9**, 6829–6838.
30 X. Ren, Y. Han, Y. Xu, T. Liu, M. Cui, L. Xia, H. Li, Y. Gu and P. Wang, Diversified strategies based on nanoscale metal–organic frameworks for cancer therapy: the leap from monofunctional to versatile, *Coord. Chem. Rev.*, 2021, **431**, 213676.
31 P. Liu, X. Xie, X. Shi, Y. Peng, J. Ding and W. Zhou, Oxygen-Self-Supplying and HIF-1α-Inhibiting Core-Shell Nanosystem for Hypoxia-Resistant Photodynamic Therapy, *ACS Appl. Mater. Interfaces*, 2019, **11**, 48261–48270.
32 R. J. Drout, L. Robison, Z. Chen, T. Islamoglu and O. K. Farha, Zirconium Metal–Organic Frameworks for Organic Pollutant Adsorption, *Trends Chem.*, 2019, **1**, 304–317.
33 J. Ma, G. Wu, S. Li, W. Tan, X. Wang, J. Li and L. Chen, Magnetic solid-phase extraction of heterocyclic pesticides in environmental water samples using metal–organic frameworks coupled to high performance liquid chromatography determination, *J. Chromatogr. A*, 2018, **1553**, 57–66.
34 W. Lu, Z. Wei, Z. Y. Gu, T. F. Liu, J. Park, J. Park, J. Tian, M. Zhang, Q. Zhang, T. Gentle, M. Bosch and H. C. Zhou, Tuning the structure and function of metal–organic frameworks via linker design, *Chem. Soc. Rev.*, 2014, **43**, 5561–5593.
35 J. R. Li, J. Sculley and H. C. Zhou, Metal–organic frameworks for separations, *Chem. Rev.*, 2012, **112**, 869–932.
36 I. Ahmed and S. H. Jhung, Composites of metal–organic frameworks: preparation and application in adsorption, *Mater. Today*, 2014, **17**, 136–146.
37 Z. Zhang, W. Sang, L. Xie and Y. Dai, Metal–organic frameworks for multimodal bioimaging and synergistic cancer chemotherapy, *Coord. Chem. Rev.*, 2019, **399**, 213022.
38 J. Yang, X. Chen, Y. Li, Q. Zhuang, P. Liu and J. Gu, Zr-Based MOFs Shielded with Phospholipid Bilayers: Improved Biostability and Cell Uptake for Biological Applications, *Chem. Mater.*, 2017, **29**, 4580–4589.
39 C. Dey, T. Kundu, B. P. Biswal, A. Mallick and R. Banerjee, Crystalline metal–Organic frameworks (MOFs): synthesis, structure and function, *Acta Crystallogr., Sect. B: Struct. Sci., Cryst. Eng. Mater.*, 2014, **70**, 3–10.
40 A. C. Tella, M. D. Olawale, M. Neuburger and J. A. Obaleye, Synthesis and crystal structure of Cd-based metal–organic framework for removal of methyl-orange from aqueous solution, *J. Solid State Chem.*, 2017, **255**, 157–166.
41 N. Stock and S. Biswas, Synthesis of Metal–Organic Frameworks (MOFs): Routes to Various MOF Topologies, Morphologies, and Composites, *Chem. Rev.*, 2012, **112**, 933–969.
42 D. T. Bankole, T. O. Abodunrin, G. O. Egharevba, A. C. Oladipo, S. O. Oladeji and O. S. Bello, Metal–organic framework for photocatalytic reduction of carbon dioxide, *Met. Fram. Nanomater. Energy Convers. Storage*, 2022, 727–748.
43 A. C. Oladipo, T. O. Abodunrin, D. T. Bankole, O. S. Oladeji, G. O. Egharevba and O. S. Bello, Environmental Applications of Metal–Organic Frameworks and Derivatives: Recent Advances and Challenges, *ACS Symp. Ser.*, 2021, **1394**, 257–298.
44 Y. Zhang, Q. Wang, G. Chen and P. Shi, DNA-Functionalized Metal–Organic Framework: Cell Imaging, Targeting Drug Delivery and Photodynamic Therapy, *Inorg. Chem.*, 2019, **58**, 6593–6596.
45 A. Bieniek, A. P. Terzyk, M. Wiśniewski, K. Roszek, P. Kowalczyk, L. Sarkisov, S. Keskin and K. Kaneko, MOF materials as therapeutic agents, drug carriers, imaging agents and biosensors in cancer biomedicine: recent advances and perspectives, *Prog. Mater. Sci.*, 2021, **117**, 100743.
46 M. Giménez-Marqués, T. Hidalgo, C. Serre and P. Horcajada, Nanostructured metal–organic frameworks and their bio-related applications, *Coord. Chem. Rev.*, 2016, **307**, 342–360.
47 T. Simon-Yarza, A. Mielcarek, P. Couvreur and C. Serre, Nanoparticles of Metal–Organic Frameworks: On the Road to In Vivo Efficacy in Biomedicine, *Adv. Mater.*, 2018, **30**, 1–15.
48 Y. Liu, Y. Zhao and X. Chen, Bioengineering of metal–organic frameworks for nanomedicine, *Theranostics*, 2019, **9**, 3122–3133.
49 X. Li, Z. Cai, L. P. Jiang, Z. He and J. J. Zhu, Metal–Ligand Coordination Nanomaterials for Biomedical Imaging, *Bioconjugate Chem.*, 2020, **31**, 332–339.
50 J. Liu, Y. Yang, W. Zhu, X. Yi, Z. Dong, X. Xu, M. Chen, K. Yang, G. Lu, L. Jiang and Z. Liu, Nanoscale metal–organic frameworks for combined photodynamic & radiation therapy in cancer treatment, *Biomaterials*, 2016, **97**, 1–9.
51 R. Chen, J. Zhang, J. Chelora, Y. Xiong, S. V. Kershaw, K. F. Li, P. K. Lo, K. W. Cheah, A. L. Rogach, J. A. Zapien and C. S. Lee, Ruthenium(II) Complex Incorporated UiO-67 Metal–Organic Framework Nanoparticles for Enhanced Two-Photon Fluorescence Imaging and Photodynamic Cancer Therapy, *ACS Appl. Mater. Interfaces*, 2017, **9**, 5699–5708.
52 O. S. Adeyemi and D. A. Otohinoyi, Inorganic nanoparticles restrict viability of metastatic breast cancer cells in vitro, *Comp. Clin. Pathol.*, 2019, **28**, 949–954.

53 M. Li, Z. Zhang, Y. Yu, H. Yuan and A. Nezamzadeh, Recent advances in Zn-MOFs and their derivatives for cancer therapeutic applications, *Mater. Adv.*, 2023, **4**, 5050–5093.
54 X. Zhang, G. Li, D. Wu, X. Li, N. Hu, J. Chen, G. Chen and Y. Wu, Recent progress in the design fabrication of metal–organic frameworks-based nanozymes and their applications to sensing and cancer therapy, *Biosens. Bioelectron.*, 2019, **137**, 178–198.
55 S. Begum, Z. Hassan, S. Bräse, C. Wöll and M. Tsotsalas, Metal–Organic Framework-Templated Biomaterials: Recent Progress in Synthesis, Functionalization, and Applications, *Acc. Chem. Res.*, 2019, **52**, 1598–1610.
56 J. Lu, X. Zhu, M. Li, C. Fu, Y. Li, J. Zhang, J. Liu and Y. Zhang, Engineering Near-Infrared-Excitable Metal–Organic Framework for Tumor Microenvironment Responsive Therapy, *ACS Appl. Bio Mater.*, 2021, **4**, 6316–6325.
57 Y. Zhang, F. Wang, C. Liu, Z. Wang, L. Kang, Y. Huang, K. Dong, J. Ren and X. Qu, Nanozyme Decorated Metal–Organic Frameworks for Enhanced Photodynamic Therapy, *ACS Nano*, 2018, **12**, 651–661.
58 M. R. Shait Mohammed, V. Ahmad, A. Ahmad, S. Tabrez, H. Choudhry, M. A. Zamzami, M. A. Bakhrebah, A. Ahmad, S. Wasi, H. Mukhtar and M. I. Khan, Prospective of nanoscale metal organic frameworks [NMOFs] for cancer therapy, *Semin. Cancer Biol.*, 2021, **69**, 129–139.
59 X. Gao, G. Ji, R. Cui and Z. Liu, Controlled synthesis of MOFs@MOFs core–shell structure for photodynamic therapy and magnetic resonance imaging, *Mater. Lett.*, 2019, **237**, 197–199.
60 K. Lu, C. He and W. Lin, A Chlorin-Based Nanoscale Metal-Organic Framework for Photodynamic Therapy of Colon Cancers, *J. Am. Chem. Soc.*, 2015, **137**(24), 7600–7603.
61 G. Lan, K. Ni, S. S. Veroneau, X. Feng, G. T. Nash, T. Luo, Z. Xu and W. Lin, Titanium-Based Nanoscale Metal–Organic Framework for Type i Photodynamic Therapy, *J. Am. Chem. Soc.*, 2019, **141**, 4204–4208.
62 M. He, Y. Chen, C. Tao, Q. Tian, L. An, J. Lin, Q. Tian, H. Yang and S. Yang, Mn–Porphyrin-Based Metal–Organic Framework with High Longitudinal Relaxivity for Magnetic Resonance Imaging Guidance and Oxygen Self-Supplementing Photodynamic Therapy, *ACS Appl. Mater. Interfaces*, 2019, **11**, 41946–41956.
63 J. L. Kan, Y. Jiang, A. Xue, Y. H. Yu, Q. Wang, Y. Zhou and Y. Bin Dong, Surface Decorated Porphyrinic Nanoscale Metal–Organic Framework for Photodynamic Therapy, *Inorg. Chem.*, 2018, **57**, 5420–5428.
64 J. Park, Q. Jiang, D. Feng, L. Mao and H. C. Zhou, Size-Controlled Synthesis of Porphyrinic Metal–Organic Framework and Functionalization for Targeted Photodynamic Therapy, *J. Am. Chem. Soc.*, 2016, **138**, 3518–3525.
65 Y. Liu, W. Hou, L. Xia, C. Cui, S. Wan, Y. Jiang, Y. Yang, Q. Wu, L. Qiu and W. Tan, ZrMOF nanoparticles as quenchers to conjugate DNA aptamers for target-induced bioimaging and photodynamic therapy, *Chem. Sci.*, 2018, **9**, 7505–7509.
66 L. Le Zhou, Q. Guan, Y. A. Li, Y. Zhou, Y. Bin Xin and Y. Bin Dong, One-Pot Synthetic Approach toward Porphyrinatozinc and Heavy-Atom Involved Zr-NMOF and Its Application in Photodynamic Therapy, *Inorg. Chem.*, 2018, **57**, 3169–3176.
67 C. Zhang, W. Chen, T. Zhang, X. Jiang and Y. Hu, Hybrid nanoparticle composites applied to photodynamic therapy: strategies and applications, *J. Mater. Chem. B*, 2020, **8**, 4726–4737.
68 K. Kim, S. Lee, E. Jin, L. Palanikumar, J. H. Lee, J. C. Kim, J. S. Nam, B. Jana, T. H. Kwon, S. K. Kwak, W. Choe and J. H. Ryu, MOF × Biopolymer: Collaborative Combination of Metal–Organic Framework and Biopolymer for Advanced Anticancer Therapy, *ACS Appl. Mater. Interfaces*, 2019, **11**, 27512–27520.
69 S. Gao, P. Zheng, Z. Li, X. Feng, W. Yan, S. Chen, W. Guo, D. Liu, X. Yang, S. Wang, X. J. Liang and J. Zhang, Biomimetic O_2-Evolving metal–organic framework nanoplatform for highly efficient photodynamic therapy against hypoxic tumor, *Biomaterials*, 2018, **178**, 83–94.
70 X. Zheng, L. Wang, Q. Pei, S. He, S. Liu and Z. Xie, Metal–Organic Framework@Porous Organic Polymer Nanocomposite for Photodynamic Therapy, *Chem. Mater.*, 2017, **29**, 2374–2381.
71 T. Luo, G. T. Nash, Z. Xu, X. Jiang, J. Liu and W. Lin, Nanoscale Metal–Organic Framework Confines Zinc-Phthalocyanine Photosensitizers for Enhanced Photodynamic Therapy, *J. Am. Chem. Soc.*, 2021, **143**, 13519–13524.
72 Y. Deng, M. Guo, L. Zhou, Y. Huang, S. Srivastava, A. Kumar and J. Liu, Prospects, advances and biological applications of MOF-based platform for the treatment of lung cancer, *Biomater. Sci.*, 2024, **12**, 3725–3744.
73 Q. Guan, L. Le Zhou, Y. A. Li and Y. Bin Dong, Diiodo-Bodipy-Encapsulated Nanoscale Metal–Organic Framework for pH-Driven Selective and Mitochondria Targeted Photodynamic Therapy, *Inorg. Chem.*, 2018, **57**, 10137–10145.
74 J. Chen, Y. Wang, H. Niu, Y. Wang, A. Wu, C. Shu, Y. Zhu, Y. Bian and K. Lin, Metal–Organic Framework-Based Nanoagents for Effective Tumor Therapy by Dual Dynamics-Amplified Oxidative Stress, *ACS Appl. Mater. Interfaces*, 2021, **13**, 45201–45213.
75 Z. Zhao, J. Ru, P. Zhou, Y. Wang, C. Shan, X. Yang, J. Cao, W. Liu, H. Guo and Y. Tang, A smart nanoprobe based on a gadolinium complex encapsulated by ZIF-8 with enhanced room temperature phosphorescence for synchronous oxygen sensing and photodynamic therapy, *Dalton Trans.*, 2019, **48**, 16952–16960.
76 Y. Zeng, J. Xiao, Y. Cong, J. Liu, Y. He, B. D. Ross, H. Xu, Y. Yin, H. Hong and W. Xu, PEGylated Nanoscale Metal–Organic Frameworks for Targeted Cancer Imaging and Drug Delivery, *Bioconjugate Chem.*, 2021, **32**, 2195–2204.
77 X. Hu, Y. Lu, L. Zhou, L. Chen, T. Yao, S. Liang, J. Han, C. Dong and S. Shi, Post-synthesis strategy to integrate porphyrinic metal–organic frameworks with CuS NPs for synergistic enhanced photo-therapy, *J. Mater. Chem. B*, 2020, **8**, 935–944.
78 C. Liu, J. Xing, O. U. Akakuru, L. Luo, S. Sun, R. Zou, Z. Yu, Q. Fang and A. Wu, Nanozymes-Engineered Metal–Organic Frameworks for Catalytic Cascades-Enhanced Synergistic Cancer Therapy, *Nano Lett.*, 2019, **19**, 5674–5682.

79 X. Cai, B. Liu, M. Pang and J. Lin, Interfacially synthesized Fe-soc-MOF nanoparticles combined with ICG for photothermal/photodynamic therapy, *Dalton Trans.*, 2018, **47**, 16329–16336.
80 X. Meng, J. Deng, F. Liu, T. Guo, M. Liu, P. Dai, A. Fan, Z. Wang and Y. Zhao, Triggered All-Active Metal Organic Framework: Ferroptosis Machinery Contributes to the Apoptotic Photodynamic Antitumor Therapy, *Nano Lett.*, 2019, **19**, 7866–7876.
81 J. Jia, Y. Zhang, M. Zheng, C. Shan, H. Yan, W. Wu, X. Gao, B. Cheng, W. Liu and Y. Tang, Functionalized Eu(III)-Based Nanoscale Metal–Organic Framework to Achieve Near-IR-Triggered and -Targeted Two-Photon Absorption Photodynamic Therapy, *Inorg. Chem.*, 2018, **57**, 300–310.
82 Q. Jiang, M. Zhang, Q. Sun, D. Yin, Z. Xuan and Y. Yang, Enhancing the Antitumor Effect of Doxorubicin with Photosensitive Metal–Organic Framework Nanoparticles against Breast Cancer, *Mol. Pharm.*, 2021, **18**, 3026–3036.
83 Q. Cheng, W. Yu, J. Ye, M. Liu, W. Liu, C. Zhang, C. Zhang, J. Feng and X. Z. Zhang, Nanotherapeutics interfere with cellular redox homeostasis for highly improved photodynamic therapy, *Biomaterials*, 2019, **224**, 119500.
84 X. Zeng, B. Chen, Y. Song, X. Lin, S. F. Zhou and G. Zhan, Fabrication of Versatile Hollow Metal–Organic Framework Nanoplatforms for Folate-Targeted and Combined Cancer Imaging and Therapy, *ACS Appl. Bio Mater.*, 2021, **4**, 6417–6429.
85 Y. T. Qin, H. Peng, X. W. He, W. Y. Li and Y. K. Zhang, PH-Responsive Polymer-Stabilized ZIF-8 Nanocomposites for Fluorescence and Magnetic Resonance Dual-Modal Imaging-Guided Chemo-/Photodynamic Combinational Cancer Therapy, *ACS Appl. Mater. Interfaces*, 2019, **11**, 34268–34281.
86 S. S. Wan, J. Y. Zeng, H. Cheng and X. Z. Zhang, ROS-induced NO generation for gas therapy and sensitizing photodynamic therapy of tumor, *Biomaterials*, 2018, **185**, 51–62.
87 J. Feng, W. Yu, Z. Xu and F. Wang, An intelligent ZIF-8-gated polydopamine nanoplatform for: *in vivo* cooperatively enhanced combination phototherapy, *Chem. Sci.*, 2020, **11**, 1649–1656.
88 P. Liu, X. Xie, X. Shi, Y. Peng, J. Ding and W. Zhou, Oxygen-Self-Supplying and HIF-1α-Inhibiting Core-Shell Nanosystem for Hypoxia-Resistant Photodynamic Therapy, *ACS Appl. Mater. Interfaces*, 2019, **11**(51), 48261–48270.
89 D. Zhang, Z. Ye, L. Wei, H. Luo and L. Xiao, Cell Membrane-Coated Porphyrin Metal–Organic Frameworks for Cancer Cell Targeting and O_2-Evolving Photodynamic Therapy, *ACS Appl. Mater. Interfaces*, 2019, **11**, 39594–39602.
90 H. Zhang and X. B. Yin, Mixed-Ligand Metal–Organic Frameworks for All-in-One Theranostics with Controlled Drug Delivery and Enhanced Photodynamic Therapy, *ACS Appl. Mater. Interfaces*, 2022, **14**, 26528–26535.
91 Y. Shao, B. Liu, Z. Di, G. Zhang, L. D. Sun, L. Li and C. H. Yan, Engineering of Upconverted Metal–Organic Frameworks for Near-Infrared Light-Triggered Combinational Photodynamic/Chemo-/Immunotherapy against Hypoxic Tumors, *J. Am. Chem. Soc.*, 2020, **142**, 3939–3946.
92 Z. Shi, K. Zhang, S. Zada, C. Zhang, X. Meng, Z. Yang and H. Dong, Upconversion Nanoparticle-Induced Multimode Photodynamic Therapy Based on a Metal–Organic Framework/Titanium Dioxide Nanocomposite, *ACS Appl. Mater. Interfaces*, 2020, **12**, 12600–12608.
93 Z. Xie, X. Cai, C. Sun, S. Liang, S. Shao, S. Huang, Z. Cheng, M. Pang, B. Xing, A. A. A. Kheraif and J. Lin, O_2-Loaded pH-Responsive Multifunctional Nanodrug Carrier for Overcoming Hypoxia and Highly Efficient Chemo-Photodynamic Cancer Therapy, *Chem. Mater.*, 2019, **31**, 483–490.